



ELSEVIER

Physica D 142 (2000) 166–196

PHYSICA D

www.elsevier.com/locate/physd

Monodromy in the hydrogen atom in crossed fields

R.H. Cushman^{a,*}, D.A. Sadovskii^b

^a *Mathematics Institute, University of Utrecht, Budapestlaan 6, 3508 TA Utrecht, The Netherlands*

^b *Université du Littoral, Citadelle, Boîte Postale 5526, 59379 Dunkirk, France*

Received 8 June 1999; received in revised form 1 February 2000; accepted 9 February 2000

Communicated by J.D. Meiss

Abstract

We show that the hydrogen atom in orthogonal electric and magnetic fields has a special property of certain integrable classical Hamiltonian systems known as monodromy. The strength of the fields is assumed to be small enough to validate the use of a truncated normal form \mathcal{H}_{snf} which is obtained from a two step normalization of the original system. We consider the level sets of \mathcal{H}_{snf} on the second reduced phase space. For an open set of field parameters we show that there is a special dynamically invariant set which is a “doubly pinched 2-torus”. This implies that the integrable Hamiltonian \mathcal{H}_{snf} has monodromy. Manifestation of monodromy in quantum mechanics is also discussed. © 2000 Elsevier Science B.V. All rights reserved.

PACS: 03.20.+i; 32.60.+i

Keywords: Singular reduction; Monodromy; Energy–momentum map

1. Introduction

Integrable Hamiltonian dynamical systems play a central role in both classical and quantum mechanics. They are used extensively to approximate many generic nonintegrable systems and their quantum analogues. Among all integrable Hamiltonian systems, the most popular are those which admit *global* action–angle coordinates and thus the invariant tori have a trivial geometry. At the same time, integrable Hamiltonian systems with more complicated toral geometry received much less attention in physics. Even when these systems appeared in applications, to a large extent their geometry remained ignored. Since the general mathematical framework for studying integrable systems with complicated geometry has been available since 1980 [1], it is now possible to close this gap and (i) to uncover geometric complexity which is *commonly* present in many physically important integrable Hamiltonian systems, (ii) to understand *inevitable* dynamical consequences of this complexity, (iii) to find its manifestation in corresponding quantum systems, and finally (iv) to extend the analysis to perturbed systems.

* Corresponding author.

E-mail addresses: cushman@math.uu.nl (R.H. Cushman), sadovski@univ-littoral.fr (D.A. Sadovskii)

This paper studies the hydrogen atom in crossed fields, a fundamental atomic system. We consider an integrable approximation. We give a detailed analysis of the geometry of this integrable approximation and show that it has a property called *monodromy* which is the simplest obstruction to the existence of global action–angle coordinates. In addition we show that monodromy is visible in the spectrum of the semiclassical quantization of the crossed fields problem.

1.1. General description

In 1980 Duistermaat [1] introduced the concept of monodromy in the study of two degrees of freedom integrable Hamiltonian systems. Since that time monodromy has been found and analysed in several integrable systems of classical mechanics [2–11]. Geometrically, monodromy describes the global twisting of a family of invariant 2-tori parameterized by a circle of regular values of the energy–momentum map of the integrable system. Its presence is signalled by the existence of a singular fiber of the energy–momentum map which is topologically a “pinched torus” [12]. Loosely speaking, if an integrable system has monodromy then it is impossible to label the tori in a unique way by values of the actions.

Since invariant tori are at the foundation of semiclassical Einstein–Brillouin–Kramers (EBK) quantization of integrable systems, monodromy should manifest itself in the corresponding quantum systems [10,11,13–16]. Because monodromy is quite common in classical integrable systems of two degrees of freedom, it should have many important physical implications in quantum mechanics.

In this paper we show that monodromy is present in the hydrogen atom in crossed magnetic and electric fields. To study monodromy, we use a *two* step normalization procedure to obtain an integrable approximation. The first step, called Keplerian normalization is well known [17–23]. We use the recent computation in [24] as our starting point. The second normalization was introduced in [25,26] for an analogous system. We focus on this step and detail a simple averaging procedure which gives principal terms necessary for the analysis of monodromy. Higher order normal form can be obtained by a more elaborate Lie series calculation [27]. Subsequently, we analyse the geometry of the integrable system associated to the integrable truncated second normal form \mathcal{H}_{snf} in order to show that, in an explicitly given open subset of relative field strengths, the Hamiltonian \mathcal{H}_{snf} has monodromy [10].

In the atom in fields problem our paper has many predecessors. In addition to the already cited work, we should mention the work on problems with axial symmetry [28,29], which implicitly uses the concept of the second reduced phase space. More importantly, we note [30–34] where the concept of a dynamical \mathbf{S}^1 symmetry (and its corresponding “third” integral) is visibly present and is used in an analysis and [35–37] and Appendix A.2 which pioneers the second normalization study of our system. We will also compare our results to the early quantum study by Solov’ev [38].¹ In Section 5, we give a detailed survey of previous work and its relation to the results of this paper. Below we provide an intuitive geometric description of monodromy.

1.2. Review of monodromy

In the past 20 years since the concept of monodromy was introduced into the study of integrable Hamiltonian systems, it has not joined the arsenal of fundamental qualitative ideas used by the physics community. Perhaps the reason for this is that monodromy uses the still insufficiently familiar ideas of global differential geometry. We hope that the following intuitive discussion will explain how one can find and analyse monodromy in an integrable system.

¹ In the notation of Solov’ev q equals our c or m , A corresponds to vector K , and I_1 and I_2 to x and y .

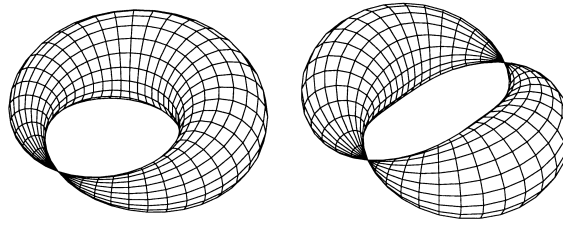


Fig. 1. Singly and doubly pinched torus: a homoclinic and heteroclinic connection of stable and unstable manifolds.

Consider a two degree of freedom Liouville integrable Hamiltonian system. It has two Poisson commuting integrals: the Hamiltonian H and a momentum J . The phase curves of this system lie on a subset of a four-dimensional phase space P . Generically, this subset is a two-dimensional torus \mathbf{T}^2 , but it can also be a point (which is an equilibrium) or a circle \mathbf{S}^1 (which is a periodic orbit).

To understand the dynamics of our system, we begin by looking at the energy–momentum map

$$\mathcal{EM} : P \rightarrow \mathbf{R}^2 : p \rightarrow (H(p), J(p)) = (h, j).$$

Corresponding to each given value (h, j) of the map \mathcal{EM} is a fiber $\mathcal{EM}^{-1}(h, j)$, which is the set of all points in phase space for which the value of \mathcal{EM} is (h, j) . We will assume that (h, j) is a *regular* value of the energy–momentum map and that the (h, j) -level set of \mathcal{EM} is compact and connected. Then the fiber $\mathcal{EM}^{-1}(h, j)$ is a smooth two-dimensional torus $T_{(h,j)}^2$. (Since this fiber is compact, by the Arnol’d–Liouville theorem [39] its connected components are two-dimensional tori.)

What we want to do is to describe how these fibers fit together as (h, j) runs over a parameterized subset of the set of regular values. Suppose that this set of regular values is a small open 2-disc D in the range of the energy–momentum map. The action–angle coordinate theorem states that $\mathcal{EM}^{-1}(D)$ (which is the union of 2-tori $T_{(h,j)}^2$, where (h, j) runs over D) has the topology of $D \times \mathbf{T}^2$. In other words,

$$\mathcal{EM}^{-1}(D) \rightarrow D : T_{(h,j)}^2 \rightarrow (h, j)$$

is a *trivial bundle* over D with total space $\mathcal{EM}^{-1}(D)$, fiber \mathbf{T}^2 , and base space D .

This simple geometric situation is greatly complicated if the 2-disc D contains a critical value $(h, j)_{\text{crit}}$ and the punctured disc $D^* = D - \{(h, j)_{\text{crit}}\}$ lies in the set of regular values in the image of \mathcal{EM} . When we are in this situation we say that the critical value $(h, j)_{\text{crit}}$ is *isolated*. Under quite general conditions the singular fiber $F = \mathcal{EM}^{-1}((h, j)_{\text{crit}})$ is a “pinched” 2-torus shown in Fig. 1. Dynamically, a singly pinched 2-torus is a homoclinic connection of stable and unstable manifolds of the pinch point, whereas a doubly pinched one is a heteroclinic connection of the stable and unstable manifolds of the two pinch points.

When the singular fiber F is a pinched 2-torus, the foliation of $\mathcal{EM}^{-1}(D^*)$ by the 2-tori $\mathcal{EM}^{-1}(h, j)$ with $(h, j) \in D^*$ is *nontrivial* [12]. This can be understood by taking a circle Γ in D^* and looking at the bundle $\Pi : \mathcal{EM}^{-1}(\Gamma) \rightarrow \Gamma$ over Γ . Geometrically, every 2-torus bundle over a circle can be obtained by the following construction. Consider the trivial 2-torus bundle $[0, 1] \times \mathbf{T}^2$ over the closed interval $[0, 1]$. Form a circle in the base of the bundle by identifying the end points of $[0, 1]$ to a single point. To obtain a 2-torus bundle over this circle identify the end 2-tori $\{0\} \times \mathbf{T}^2$ and $\{1\} \times \mathbf{T}^2$ by an invertible map $M : \mathbf{T}^2 \rightarrow \mathbf{T}^2$, called the *monodromy map*. This map glues the end tori together after giving them a twist. For a lower dimensional example of this twisting construction, think of a cylinder and a Möbius band. Start with a product of $[0, 1]$ and an open interval (which is a trivial bundle over $[0, 1]$). A cylinder is formed by gluing the open intervals over the end points by the identity map, while the Möbius band is formed by using minus the identity as the gluing map.

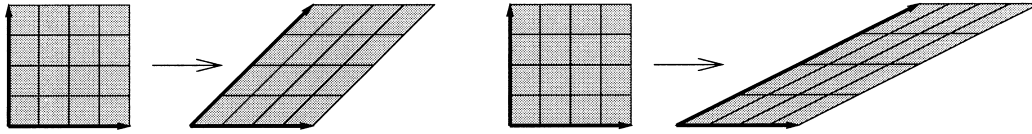


Fig. 2. Monodromy map $\mathcal{EM}^{-1}(p_0) \rightarrow \mathcal{EM}^{-1}(p_1) : L_{p_0} \rightarrow L_{p_1}$ identifying once (left) and twice (right) twisted end 2-torus $\mathcal{EM}^{-1}(p_1)$ and initial 2-torus $\mathcal{EM}^{-1}(p_0)$.

We return to considering our 2-torus bundle Π over the circle Γ . Here is a theoretical method for computing its monodromy map. Cut the circle Γ at a point p and think of it as an interval whose closure \mathcal{I} has end points p_0 and p_1 . Cover the interval \mathcal{I} by a finite set of pairwise overlapping intervals \mathcal{I}_i on which the local actions given by the action–angle coordinate theorem are defined. On the overlap $\mathcal{I}_i \cap \mathcal{I}_{i+1}$ adjust the actions so that they agree. As a result of this construction we have found the values $(j_1^{p_1}, j_2^{p_1})$ of the actions at p_1 starting with their values at $(j_1^{p_0}, j_2^{p_0})$ at p_0 by following the curve $\Gamma - \{p\}$. Care is needed because, as functions on the set of regular values of the energy–momentum map, the actions (j_1, j_2) may be *multi-valued*. The actions $(j_1^{p_i}, j_2^{p_i})$ label the 2-torus $\mathcal{EM}^{-1}(p_i)$ for $i = 1, 2$. We think of the 2-torus $\mathcal{EM}^{-1}(p_0)$ as the space \mathbf{R}^2/L_{p_0} , where L_{p_0} is the lattice generated by evaluating the Hamiltonian vector fields $X_{j_i^{p_0}}$ corresponding to the action $j_i^{p_0}$ at the point p_0 . (In other words, two vectors in \mathbf{R}^2 represent the same point on the 2-torus $\mathcal{EM}^{-1}(p_0)$ if their coordinates differ by some *integer* linear combination of vectors in L_{p_0} .) Similarly, the 2-torus $\mathcal{EM}^{-1}(p_1)$ is \mathbf{R}^2/L_{p_1} . Consider the invertible linear map M which assigns to the generators of L_{p_0} the generators of L_{p_1} (see Fig. 2). The map M is given by an integer 2×2 matrix with determinant 1, which maps the 2-torus $\mathcal{EM}^{-1}(p_0)$ onto the 2-torus $\mathcal{EM}^{-1}(p_1)$. Of course the torus $\mathcal{EM}^{-1}(p_1)$ is the same as the torus $\mathcal{EM}^{-1}(p_0)$. Thus, M is the monodromy map of the bundle Π . It is a theorem [40] that M has the form

$$\begin{pmatrix} 1 & k \\ 0 & 1 \end{pmatrix},$$

where k is the number of pinch points of the singular fiber F . From the above discussion it is clear that the monodromy matrix determines the global geometry of the 2-torus bundle around a pinched 2-torus singular fiber F of the energy–momentum mapping.

1.3. More detailed description

We continue this introduction with a precise description of the crossed fields problem and give an outline of the geometry of this system.

1.3.1. Hydrogen atom in orthogonal external fields

The Hamiltonian function of the hydrogen atom in the presence of constant orthogonal magnetic and electric fields^{2,3} is

$$H = \frac{1}{2}P^2 - \frac{C}{r} + FQ_2 + \frac{1}{2}G(Q_2P_3 - Q_3P_2) + \frac{1}{8}G^2(Q_2^2 + Q_3^2) \tag{1}$$

with subscripts (1,2,3) equal to (b,e,p) of Ref. [24]. The direction of the magnetic and electric fields are, respectively, 1 and 2; Q_s are the coordinates in physical 3-space, P is the 3-vector of conjugate momenta, and $r = |Q|$ is the

² We ignore all effects due to the spin of the electron, relativistic corrections, and we also simplify the two-body problem by considering an infinitely heavy nucleus (while in reality $m_p/m_e \approx 1836$).

³As in [24] and elsewhere we use atomic units.

3-space length of Q . The first two terms in the right-hand side of (1) represent the Kepler Hamiltonian, the third is the electrostatic potential describing Stark effect, and the two last terms describe the linear and quadratic Zeeman effect. We introduce an “effective charge” C in order to have the same kind of parameters as in (1.1) of Ref. [25]. The Hamiltonian in [25] is equivalent to (1) with the quadratic Zeeman term omitted and thus can be interpreted as a case when the magnetic field strength G is small.

For $F \neq 0$ and $G \neq 0$ the Hamiltonian function H (1) has no strict continuous symmetry. However, it does have a discrete $\mathbf{Z}_2 \times \mathbf{Z}_2$ symmetry which will be taken into account in our analysis. More information on the symmetry analysis can be found in Refs. [24,27].

1.3.2. Scheme of the analysis and geometry

To determine whether our Hamiltonian system has monodromy, we normalize H (1) *twice* and study the resulting integrable system. First we normalize H w.r.t. the Keplerian symmetry. Truncating at order 2 gives the first normal form \mathcal{H}_{nf} which has the regularized Kepler Hamiltonian $H_0 = 2N$ as an integral of motion. (For our original Hamiltonian system $2N$ is an approximate integral of motion). Removing the Keplerian symmetry from the first normal form gives a two degree of freedom Hamiltonian system on $S_{n/2}^2 \times S_{n/2}^2$, the product of two 2-spheres of radius $n/2$. Here n is the value of the Keplerian integral N . The coordinates used to describe the first reduced phase space $S_{n/2} \times S_{n/2}$ are the Hamiltonian functions corresponding to the vector fields generating the SO(4) symmetry of H_0 .

To perform the second normalization we look at the first order term \mathcal{H}_1 in \mathcal{H}_{nf} . Using the Poisson structure of the $S_{n/2}^2 \times S_{n/2}^2$ coordinate functions, we obtain a Hamiltonian vector field $X_{\mathcal{H}_1}$ on $S_{n/2}^2 \times S_{n/2}^2$ whose flow generates an \mathbf{S}^1 symmetry. This is an approximate symmetry of the first normal form. Averaging \mathcal{H}_{nf} w.r.t. to the flow of $X_{\mathcal{H}_1}$ gives the second normal form \mathcal{H}_{snf} . Note that \mathcal{H}_1 is an integral of the Hamiltonian system corresponding to the second normal form. We then investigate the geometry of the level sets of the energy–momentum mapping

$$\mathcal{EM} : S_{n/2}^2 \times S_{n/2}^2 \rightarrow \mathbf{R}^2 : p \rightarrow (\mathcal{H}_{\text{snf}}(p), \mathcal{H}_1(p))$$

by reducing the \mathbf{S}^1 symmetry to obtain a one degree of freedom system on $P_{n,c}$. Because the \mathbf{S}^1 action on $M_c = \mathcal{H}_{\text{nf}}^{-1}(c) \cap (S_{n/2}^2 \times S_{n/2}^2)$ defined by the flow of $X_{\mathcal{H}_1}$ has fixed points when $c = 0$ and $c = \pm n$, we must use *singular reduction* [2] to obtain the second reduced phase space $P_{n,c}$. We show that for an explicitly given open set of field parameters the (0,0)-level set of \mathcal{EM} (i.e., the set of all points in $S_{n/2}^2 \times S_{n/2}^2$, where \mathcal{H}_1 and \mathcal{H}_{snf} both take the value 0), is a doubly pinched 2-torus in $S_{n/2}^2 \times S_{n/2}^2$. It follows that the energy–momentum map \mathcal{EM} has monodromy (see [12]).

2. Review of first normal form

This section reviews the familiar grounds for obtaining the first normal form. Our treatment follows [24] and explains the details of the field strength scaling. More explanation of the computation of the first normal form, its finite symmetries and its expression in terms of the SO(4) symmetry generators can be found in [24,27].

2.1. Regularization and rescaling

In order to perform normalization one needs to regularize the Hamiltonian (1) so that its bounded orbits are defined for all time. Intuitively speaking, regularization removes the $1/r$ singularity from the Kepler Hamiltonian.

First we fix a value $E < 0$ of the energy. We then rescale length and momentum by $(Q, P) \rightarrow (C^{-1}Q, CP)$ so that the effective charge C in (1) becomes 1. After rescaling time by $t \rightarrow C^2t$, the Hamiltonian (1) becomes

$$0 = \frac{1}{2}P^2 - \frac{1}{|Q|} - \frac{E}{C^2} + \frac{F}{C^3}Q_2 + \frac{G}{2C^2}(Q_2P_3 - Q_3P_2) + \frac{G^2}{8C^4}(Q_2^2 + Q_3^2). \quad (2a)$$

Next we define a new timescale by $dt \rightarrow (1/|Q|) dt$. Eq. (2a) becomes

$$0 = \frac{1}{2}|Q| \left(P^2 - \frac{2E}{C^2} \right) - 1 + \frac{F}{C^3}Q_2|Q| + \frac{G}{2C^2}(Q_2P_3 - Q_3P_2)|Q| + \frac{G^2}{8C^4}(Q_2^2 + Q_3^2)|Q|. \quad (2b)$$

We now regularize (2b) using the method of Kustaanheimo and Stiefel (KS). The KS method lifts the phase space $T_0\mathbf{R}^3 = (\mathbf{R}^3 - \{0\}) \times \mathbf{R}^3$ (with canonical coordinates (Q, P)) to the larger phase space $T_0\mathbf{R}^4 = (\mathbf{R}^4 - \{0\}) \times \mathbf{R}^4$ (with canonical coordinates (q, p)) using the mapping

$$\text{KS} : T_0\mathbf{R}^4 \rightarrow T_0\mathbf{R}^3 : (q, p) \rightarrow \left(M_{\text{KS}}(q), \frac{M_{\text{KS}}(p)}{r} \right) = (Q, 0, P, 0). \quad (3)$$

Here

$$M_{\text{KS}} = \begin{pmatrix} q_1 & -q_2 & -q_3 & q_4 \\ q_2 & q_1 & -q_4 & -q_3 \\ q_3 & q_4 & q_1 & q_2 \\ q_4 & -q_3 & q_2 & -q_1 \end{pmatrix}, \quad r = |Q| = q^2.$$

In defining the KS map (3) we require

$$\zeta = q_1p_4 - q_2p_3 + q_3p_2 - q_4p_1 = 0. \quad (4)$$

Using the KS map, Eq. (2b) becomes

$$1 = \frac{1}{2} \left(\frac{1}{4}p^2 + \frac{-2E}{C^2}q^2 \right) + \frac{2F}{C^3}(q_1q_2 - q_3q_4)q^2 + \frac{G}{2C^2}(q_2p_3 - q_3p_2)q^2 + \frac{G^2}{8C^4}(q_1^2 + q_4^2)(q_2^2 + q_3^2)q^2. \quad (5)$$

After rescaling the variables q and p by $(q, p) \rightarrow (q/\sqrt{\omega}, p\sqrt{\omega})$, where $\omega = 2\sqrt{-2K}/C$, and rescaling time by $t \rightarrow \frac{1}{4}\omega t$, Eq. (5) becomes

$$\frac{4}{\omega} = H = \frac{1}{2}(p^2 + q^2) + \frac{1}{3}f(q_1q_2 - q_3q_4)^2q^2 + \frac{1}{2}g(q_2p_3 - q_3p_2)q^2 + \frac{1}{8}g^2(q_1^2 + q_4^2)(q_2^2 + q_3^2)q^2. \quad (6)$$

Choosing the scaled field parameters as

$$f = 3F \left(\frac{2}{C\omega} \right)^3 = \varepsilon\beta, \quad g = G \left(\frac{2}{C\omega} \right)^2 = \varepsilon\alpha,$$

where α and β are two dimensionless parameters satisfying

$$\alpha \geq 0, \quad \beta \geq 0, \quad \alpha^2 + \beta^2 = 1 \quad (7)$$

and ε is a smallness parameter [24],⁴ the Hamiltonian H (6) can be written as

$$\begin{aligned} H(q, p) &= \frac{1}{2}(p^2 + q^2) + \varepsilon(\beta(q_1q_2 - q_3q_4)^2 + \alpha(q_2p_3 - q_3p_2))q^2 + \frac{1}{2}\varepsilon^2(\frac{1}{4}\alpha^2(q_1^2 + q_4^2)(q_2^2 + q_3^2)q^2) \\ &= H_0 + \varepsilon H_1 + \frac{1}{2}\varepsilon^2 H_2, \end{aligned} \quad (8)$$

which is a perturbation of the 1:1:1:1 harmonic oscillator. Note that the KS function (4) is an integral of the Hamiltonian vector field X_H .

2.2. Normalization and reduction

Having written the Hamiltonian (8) as a perturbation of the harmonic oscillator H_0 , we can carry out its normalization using standard Lie series methods. This normalization procedure gives a canonical coordinate change on $T\mathbf{R}^4$ for which the transformed Hamiltonian Poisson commutes with H_0 up through second order terms in ε . The truncated normalized Hamiltonian

$$\mathcal{H}_{\text{inf}} = H_0 + \varepsilon \mathcal{H}_1 + \frac{1}{2}\varepsilon^2 \mathcal{H}_2 \quad (9)$$

also Poisson commutes with the KS integral ζ (4) because the normalizing coordinate change commutes with the \mathbf{S}^1 symmetry of H (8) generated by the flow of X_ζ . Thus, \mathcal{H}_{inf} is invariant under the \mathbf{T}^2 symmetry generated by H_0 and ζ .

The algebra of polynomials on $T\mathbf{R}^4$ which are invariant under this \mathbf{T}^2 action is generated by

$$K_1 = \frac{1}{4}[p_2^2 + q_2^2 + p_3^2 + q_3^2 - (p_1^2 + q_1^2) - (p_4^2 + q_4^2)], \quad (10a)$$

$$K_2 = \frac{1}{4}(p_3p_4 - q_1q_2 - p_1p_2 + q_3q_4), \quad (10b)$$

$$K_3 = -\frac{1}{2}(q_1q_3 + q_2q_4 + p_1p_3 + p_2p_4), \quad (10c)$$

$$L_1 = \frac{1}{2}(q_2p_3 - q_3p_2 + q_1p_4 - q_4p_1), \quad (10d)$$

$$L_2 = \frac{1}{2}(q_2p_4 + q_3p_1 - q_1p_3 - q_4p_2), \quad (10e)$$

$$L_3 = \frac{1}{2}(q_1p_2 + q_3p_4 - q_2p_1 - q_4p_3), \quad (10f)$$

together with H_0 and ζ . The vectors $K = (K_1, K_2, K_3)$ and $L = (L_1, L_2, L_3)$ are nothing but the modified eccentricity⁵ and angular momentum vectors for the Kepler Hamiltonian written in terms of the KS variables (q, p) . The above \mathbf{T}^2 -invariants satisfy two relations

$$K \cdot K + L \cdot L = \frac{1}{4}H_0^2, \quad K \cdot L = 0. \quad (11)$$

Thus the space of \mathbf{T}^2 orbits on $H_0^{-1}(2n) \cap \zeta^{-1}(0)$ is defined by

$$K^2 + L^2 = n^2, \quad K \cdot L = 0. \quad (12a)$$

Since (12a) is equivalent to

$$(K + L)^2 = n^2, \quad (K - L)^2 = n^2, \quad (12b)$$

⁴ In the notation of [24] $\alpha = G_s$, $\beta = F_s$ and $\varepsilon = \tau/n = S(\omega/2)$, where $S = C(2/C\omega)^2\sqrt{G^2 + (3F(2/C\omega))^2}$ is the scaled uniform field intensity used as a smallness parameter. In [24] the symmetry group $\mathbf{Z}_2 \times \mathbf{Z}_2$ with operations $(e, \sigma_1, \sigma_2, \sigma_3)$ is called G_4 with operations (I, T_2, σ, T_3) .

⁵ Often called after Laplace–Runge–Lenz, see [2], p. 400, note to p. 55.

the \mathbf{T}^2 -orbit space is the product of two 2-spheres $S_{n/2}^2 \times S_{n/2}^2$. The Poisson structure on $S_{n/2}^2 \times S_{n/2}^2$ is determined by the $\mathfrak{so}(4)$ relations

$$\{L_i, L_j\} = \varepsilon_{ijk} L_k, \quad \{K_i, K_j\} = \varepsilon_{ijk} L_k, \quad \{L_i, K_j\} = \varepsilon_{ijk} K_k. \quad (13)$$

In [24] the first normalized Hamiltonian \mathcal{H}_{fnf} in (9) is expressed in terms of \mathbf{T}^2 -invariant polynomials restricted to $S_{n/2}^2 \times S_{n/2}^2$. Rescaling time by $t \rightarrow -tn$ and dropping the additive constant $(3\alpha^2 - 17\beta^2/9) \varepsilon/4$, we can write \mathcal{H}_{fnf} as

$$H_0 = 2, \quad (14a)$$

$$\mathcal{H}_1 = \alpha L_1 + \beta K_2, \quad (14b)$$

$$\mathcal{H}_2 = \frac{1}{4}\alpha^2[3L_1^2 + 2L_2^2 + 3K_1^2 - 2K_2^2 + 2(L_3^2 - K_3^2)] + \frac{1}{3}\alpha\beta(7K_2L_1 - L_2K_1) + \frac{1}{12}\beta^2(17K_2^2 - 3L_2^2). \quad (14c)$$

3. Second normal form

In this section we show how to normalize the Hamiltonian \mathcal{H}_{fnf} of the first normal form once again using the \mathbf{S}^1 symmetry generated by \mathcal{H}_1 . We then reduce this \mathbf{S}^1 symmetry to obtain a one degree of freedom Hamiltonian $\mathcal{H}_{n,c}$ on a possibly singular second reduced phase space $P_{n,c}$. When $c = 0$ we analyse the geometry of this one degree of freedom system $\mathcal{H}_{n,0}$ on the singular space $P_{n,0}$. We find an open interval of values of the parameter α such that the energy–momentum map $(\mathcal{H}_{\text{snf}}, \mathcal{H}_1)$ has monodromy.

3.1. Calculation of the second normal form

In order to calculate the second normal form for \mathcal{H}_{fnf} in (14a)–(14c), we make its first order term $\mathcal{H}_1 = \alpha L_1 + \beta K_2$ the first basis element of the $\mathfrak{so}(4)$ Poisson algebra (13). To do this we use the fact that $\alpha^2 + \beta^2 = 1$ and define a Poisson automorphism $(L, K) \rightarrow (T, V)$ with

$$(T, V) = \left(\left(\begin{array}{c} \alpha L_1 + \beta K_2 \\ \alpha L_2 - \beta K_1 \\ L_3 \end{array} \right), \left(\begin{array}{c} \beta L_2 + \alpha K_1 \\ \alpha K_2 - \beta L_1 \\ K_3 \end{array} \right) \right). \quad (15)$$

Of course, the Poisson brackets for the components of T and V are the same as in (13) with L and K replaced by T and V , respectively. We can also work directly with the Poisson algebra generated by the components of $x = \frac{1}{2}(T + V)$ and $y = \frac{1}{2}(T - V)$, namely

$$x_1 = \frac{1}{2}(T_1 + V_1), \quad x_2 = \frac{1}{2}(T_2 + V_2), \quad x_3 = \frac{1}{2}(T_3 + V_3), \quad (16a)$$

$$y_1 = \frac{1}{2}(T_1 - V_1), \quad y_2 = \frac{1}{2}(T_2 - V_2), \quad y_3 = \frac{1}{2}(T_3 - V_3). \quad (16b)$$

In terms of these variables, the first reduced phase space $S_{n/2}^2 \times S_{n/2}^2$ is defined by the Casimirs

$$x_1^2 + x_2^2 + x_3^2 = \frac{1}{4}n^2, \quad y_1^2 + y_2^2 + y_3^2 = \frac{1}{4}n^2, \quad (17)$$

and the Poisson bracket satisfies the $\mathfrak{so}(3) \times \mathfrak{so}(3)$ relations

$$\{x_i, x_j\} = \varepsilon_{ijk} x_k, \quad \{y_i, y_j\} = \varepsilon_{ijk} y_k, \quad \{x_i, y_j\} = 0. \quad (18)$$

After dropping the constant $H_0 = 2$, rescaling the time by $t \rightarrow \varepsilon t$, and then changing to variables (x, y) , the first normalized Hamiltonian (9) up to first order becomes

$$\mathcal{H}_{\text{inf}} = \mathcal{H}_1 + \frac{1}{2}\varepsilon\mathcal{H}_2 = T_1 + \frac{1}{2}\varepsilon\mathcal{H}_2 = (x_1 + y_1) + \frac{1}{2}\varepsilon\mathcal{H}_2, \quad (19a)$$

where

$$\begin{aligned} \mathcal{H}_2 = & \frac{1}{3}(2\alpha^4 - \alpha^2 + \frac{7}{2})(x_1^2 + y_1^2) + \frac{2}{3}\alpha^2(1 - \alpha^2)(x_2^2 + y_2^2) + \frac{1}{3}\alpha\beta(1 - 4\alpha^2)(x_1x_2 - y_1y_2) \\ & + \frac{2}{3}\alpha\beta(x_2y_1 - x_1y_2) + 2\alpha^2(x_2y_2 + x_3y_3) + \frac{10}{3}(1 - \alpha^2)x_1y_1. \end{aligned} \quad (19b)$$

The vector field

$$X_{\mathcal{H}_1} = -T_3 \frac{\partial}{\partial T_2} + T_2 \frac{\partial}{\partial T_3} - V_3 \frac{\partial}{\partial V_2} + V_2 \frac{\partial}{\partial V_3} \quad (20a)$$

$$= -x_3 \frac{\partial}{\partial x_2} + x_2 \frac{\partial}{\partial x_3} - y_3 \frac{\partial}{\partial y_2} + y_2 \frac{\partial}{\partial y_3} \quad (20b)$$

has flow given by

$$\varphi_t(x, y) = (R_t x, R_t y), \quad R_t = \begin{pmatrix} 1 & 0 & 0 \\ 0 & \cos t & -\sin t \\ 0 & \sin t & \cos t \end{pmatrix}. \quad (21)$$

In other words, φ_t defines an \mathbf{S}^1 action on $\mathbf{R}^3 \times \mathbf{R}^3$ which satisfies $\varphi_{2\pi} = \text{id}$ and leaves the first reduced phase space $S_{n/2}^2 \times S_{n/2}^2$ invariant. Thus, we may normalize \mathcal{H}_{inf} a second time. This can be done by a simple averaging of \mathcal{H}_2 along the orbits of $X_{\mathcal{H}_1}$ namely

$$\bar{\mathcal{H}}_2(x, y) = \frac{1}{2\pi} \int_0^{2\pi} \mathcal{H}_2(\varphi_t(x, y)) dt. \quad (22)$$

Thus to first order the second normalized Hamiltonian is

$$\mathcal{H}_{\text{snf}} = \mathcal{H}_1 + \frac{1}{2}\varepsilon\bar{\mathcal{H}}_2, \quad (23a)$$

with

$$\bar{\mathcal{H}}_2(x, y) = \frac{1}{3}(2\alpha^4 - \alpha^2 + \frac{7}{2})(x_1^2 + y_1^2) + \frac{1}{3}\alpha^2\beta^2(x_2^2 + x_3^2 + y_2^2 + y_3^2) + \frac{10}{3}\beta^2x_1y_1 + 2\alpha^2(x_2y_2 + x_3y_3). \quad (23b)$$

This can be further simplified using (7) and (17) to

$$\bar{\mathcal{H}}_2(x, y) = (\alpha^4 - \frac{2}{3}\alpha^2 + \frac{7}{6})(x_1^2 + y_1^2) + \frac{1}{6}n^2\alpha^2\beta^2 + \frac{10}{3}\beta^2x_1y_1 + 2\alpha^2(x_2y_2 + x_3y_3). \quad (23c)$$

The normal form \mathcal{H}_{snf} retains only those terms $\pi(x, y)$ of \mathcal{H}_2 (a homogeneous polynomial in (x, y) of degree 2) which Poisson commute with \mathcal{H}_1 , i.e., for which $X_{\mathcal{H}_1}(\pi(x, y)) = 0$. Since $\bar{\mathcal{H}}_2$ is constant on the integral curves of $X_{\mathcal{H}_1}$, it follows that \mathcal{H}_1 is a second integral of $X_{\mathcal{H}_{\text{snf}}}$. Thus $(\mathcal{H}_{\text{snf}}, \mathcal{H}_1)$ is a Liouville integrable system on the first reduced phase space $S_{n/2}^2 \times S_{n/2}^2$ with coordinates (x, y) and Poisson bracket (18). The energy–momentum map for this integrable system is

$$\mathcal{EM} : S_{n/2}^2 \times S_{n/2}^2 \rightarrow \mathbf{R}^2 : p \rightarrow (\mathcal{H}_{\text{snf}}(p), \mathcal{H}_1(p)). \quad (24)$$

3.2. Reduction to one degree of freedom

Here, we analyse the integrable system $(\mathcal{H}_{\text{snf}}, \mathcal{H}_1)$ by reducing the \mathbf{S}^1 symmetry generated by \mathcal{H}_1 using the method of *singular reduction* [2,25]. We thereby obtain a one degree of freedom system.

3.2.1. Second reduced phase space

First we use invariant theory to construct the second reduced space. The algebra of polynomials on $\mathbf{R}^3 \times \mathbf{R}^3$ which are invariant under the \mathbf{S}^1 action defined by φ_t (21) is generated by

$$\pi_1 = x_1 - y_1 = V_1, \quad (25a)$$

$$\pi_2 = 4(x_2y_2 + x_3y_3) = T_2^2 + T_3^2 - V_2^2 - V_3^2, \quad (25b)$$

$$\pi_3 = 4(x_3y_2 - x_2y_3) = 2(T_2V_3 - T_3V_2), \quad (25c)$$

$$\pi_4 = x_1 + y_1 = T_1, \quad (25d)$$

$$\pi_5 = 4(x_2^2 + x_3^2), \quad (25e)$$

$$\pi_6 = 4(y_2^2 + y_3^2), \quad (25f)$$

subject to the relation

$$\pi_2^2 + \pi_3^2 = \pi_5\pi_6, \quad \pi_5, \pi_6 \geq 0. \quad (26)$$

Eq. (26) defines the space of φ_t orbits on $\mathbf{R}^3 \times \mathbf{R}^3$. To find an explicit defining relation for the second reduced phase space we note that the c -level set of \mathcal{H}_1 , which is given by

$$\mathcal{H}_1 = T_1 = x_1 + y_1 = c, \quad |c| \leq n, \quad (27)$$

and (17), is a φ_t -invariant submanifold M_c of $S_{n/2}^2 \times S_{n/2}^2 \subset \mathbf{R}^3 \times \mathbf{R}^3$. The second reduced phase space $P_{n,c}$ is the space of φ_t orbits on M_c and is defined in terms of invariant polynomials (25a)–(25f) by

$$\pi_4 = c, \quad (28a)$$

$$\pi_5 = n^2 - (\pi_1 + \pi_4)^2, \quad (28b)$$

$$\pi_6 = n^2 - (\pi_4 - \pi_1)^2, \quad (28c)$$

$$\pi_2^2 + \pi_3^2 = \pi_5\pi_6, \quad \pi_5, \pi_6 \geq 0. \quad (28d)$$

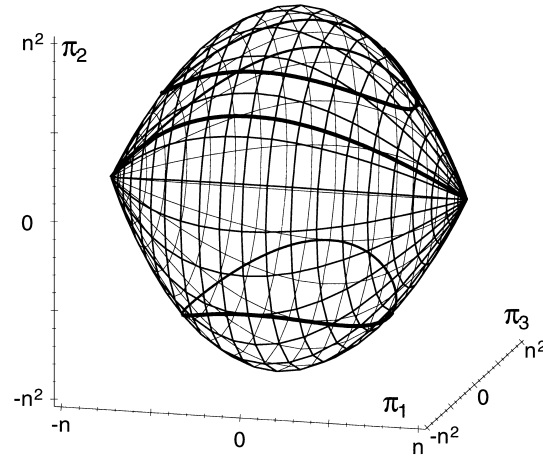
(Eqs. (28a)–(28c) come from expressing the defining equations (17) and (27) of M_c in terms of invariant polynomials (25a)–(25f). These equations are complemented by the relation (26)). Using the relations in (28a)–(28d) to eliminate the variables π_4 , π_5 , and π_6 , we see that $P_{n,c}$ is the semialgebraic variety defined in \mathbf{R}^3 with coordinates (π_1, π_2, π_3) by

$$\pi_2^2 + \pi_3^2 = [(n - c)^2 - \pi_1^2][(n + c)^2 - \pi_1^2]. \quad (29a)$$

The values of π_1 , π_2 , and π_3 in (29a) are subject to the restrictions

$$|\pi_1| \leq n - |c|, \quad |\pi_2| \leq n^2 - c^2, \quad |\pi_3| \leq n^2 - c^2. \quad (29b)$$

(The first restriction follows from the fact that for any $|c| \leq n$ and $|\pi_1| \leq n$, use (17)) the two factors on the right-hand side of (29a) cannot be both negative and hence they should be both positive.) From (29a) and (29b) we

Fig. 3. The second reduced phase space $P_{n,0}$.

can see that when $0 < |c| < n$, the second reduced phase space is a smooth 2-sphere; when $|c| = n$ it is a point; when $c = 0$ it is a topological 2-sphere with two conical singular points shown in Fig. 3. The reason why $P_{n,0}$ has two singular points is that the \mathbf{S}^1 action φ_t on M_0 has two fixed points $(x, y) = \frac{1}{2}n(\pm 1, 0, 0, \mp 1, 0, 0)$. (The two other fixed points of the φ_t action on $S_{n/2}^2 \times S_{n/2}^2$ are $(x, y) = \pm \frac{1}{2}n(1, 0, 0, 1, 0, 0)$ corresponding to $P_{n,\pm n}$, see [24,27] for more details.)

3.2.2. Reduction of finite symmetries

As discussed in Ref. [24], the original Hamiltonian H (1) has two distinct \mathbf{Z}_2 symmetries: one given by the composition of momentum reversal $(Q, P) \rightarrow (Q, -P)$ and rotation through π around axis Q_2 of the electric field F

$$\sigma_1 : (Q, P) \rightarrow (-Q_1, Q_2, -Q_3, P_1, -P_2, P_3),$$

and the other given by a reflection in the plane orthogonal to axis Q_1 of the magnetic field G

$$\sigma_2 : (Q, P) \rightarrow (-Q_1, Q_2, Q_3, -P_1, P_2, P_3).$$

The two \mathbf{Z}_2 actions commute and the total finite symmetry group of (1) is the group $\mathbf{Z}_2 \times \mathbf{Z}_2$ of order 4. Its third nontrivial operation is

$$\sigma_3 : (Q, P) \rightarrow (Q_1, Q_2, -Q_3, -P_1, -P_2, P_3),$$

which is the composition of the momentum reversal and reflection in the plane spanned by the electric and magnetic field vectors, see Fig. 4. Tracing these symmetries through the two reduction steps, we find that their action on the invariants π_k in (25a)–(25f) (and thus on the second reduced phase space $P_{n,c}$) is given by

$$\sigma_1 : (\pi_1, \pi_2, \pi_3) \rightarrow (-\pi_1, \pi_2, \pi_3), \quad (30a)$$

$$\sigma_2 : (\pi_1, \pi_2, \pi_3) \rightarrow (-\pi_1, \pi_2, -\pi_3), \quad (30b)$$

$$\sigma_3 : (\pi_1, \pi_2, \pi_3) \rightarrow (\pi_1, \pi_2, -\pi_3). \quad (30c)$$

The orbit map of the \mathbf{Z}_2 subgroup generated by (30a) is given by $(\pi_1, \pi_2, \pi_3) \rightarrow (w, \pi_2, \pi_3)$, where

$$w = (n - |c|)^2 - \pi_1^2. \quad (31)$$

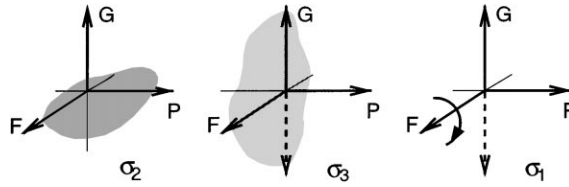


Fig. 4. Action of the symmetry operations of the $\mathbf{Z}_2 \times \mathbf{Z}_2$ finite symmetry group of the hydrogen atom in orthogonal fields on the vectors of electric and magnetic fields F and G . (Position of G obtained without momentum reversal which sends $G \rightarrow -G$ is shown by the dashed line.)

Thus the image of $P_{n,c}$ under (31) is the semialgebraic variety $V_{n,c}$ defined in \mathbf{R}^3 (with coordinates (w, π_2, π_3)) by

$$\pi_2^2 + \pi_3^2 = w(w + 2n|c|), \quad 0 \leq w \leq (n - |c|)^2. \tag{32}$$

When $0 < |c| < n$, $V_{n,c}$ is a smooth manifold with boundary at $w = (n - |c|)^2$ which is diffeomorphic to a closed 2-disc; when $|c| = n$ it is a point; when $c = 0$, the variety $V_{n,0}$ is a topological closed 2-disc with a conical singular point, see Fig. 5. The remaining \mathbf{Z}_2 symmetries (30b) and (30c) induce a \mathbf{Z}_2 action on $V_{n,c}$ generated by

$$(w, \pi_2, \pi_3) \rightarrow (w, \pi_2, -\pi_3).$$

The orbit space $V_{n,c}^0$ of this \mathbf{Z}_2 action on $V_{n,c}$ is the projection of $V_{n,c}$ on the $\{\pi_3 = 0\}$ plane (see Fig. 5, right), i.e., $V_{n,c}^0$ is the image of the map

$$V_{n,c} \rightarrow \{\pi_3 = 0\} : (w, \pi_2, \pi_3) \rightarrow (w, \pi_2, 0).$$

We call the space $V_{n,c}^0$ the *full symmetry reduced space* of the second normal form. For comparison with earlier work [25,26], we will also use $P_{n,c}^0$ which is the projection of the second reduced space $P_{n,c}$ (Fig. 3) on the $\{\pi_3 = 0\}$ plane.

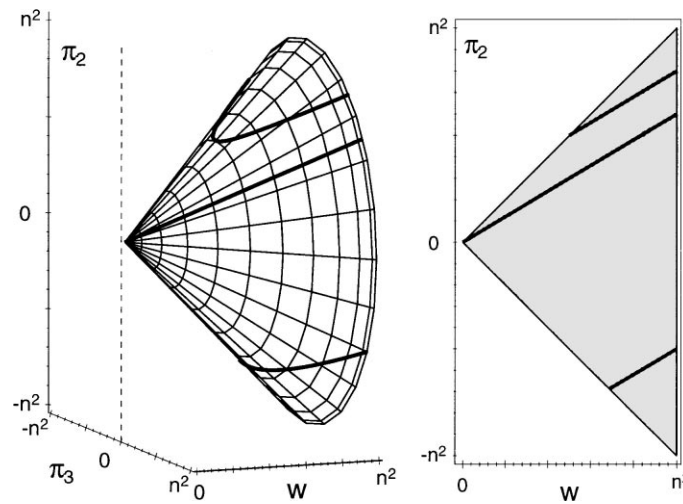


Fig. 5. The variety $V_{n,0}$ (left) obtained as the orbit space of the \mathbf{Z}_2 action (30a) on the second reduced phase space $P_{n,0}$. Fully symmetry reduced phase space $V_{n,0}^0$ (right) obtained as the orbit space of the $\mathbf{Z}_2 \times \mathbf{Z}_2$ action (30a)–(30c) on the second reduced phase space $P_{n,0}$ in Fig. 3. $V_{n,0}^0$ is a projection of the variety $V_{n,0}$ (left) on the $\pi_3 = 0$ plane.

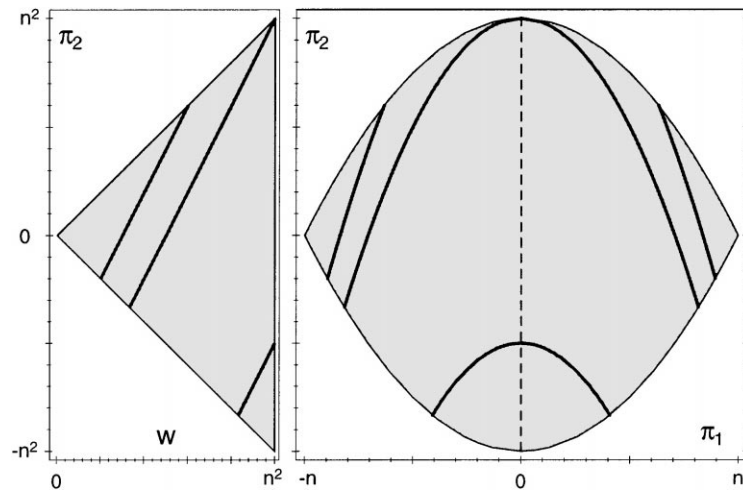


Fig. 6. Constant level sets of $\tilde{\mathcal{H}}_{n,0}$ on $V_{n,0}^0$ (left) and on $P_{n,0}^0$ (right) in the case when $|b/a| > 1$ (without monodromy).

3.2.3. Reduced second normal form

The second normal form and the manifold M_c are invariant under the action φ_t (21). The restriction of \mathcal{H}_{snf} (23a)–(23c) descends to a function $\mathcal{H}_{n,c}$ on $P_{n,c}$, called the reduced second normal form. Furthermore, the function $\mathcal{H}_{n,c}$ is invariant w.r.t. the $\mathbf{Z}_2 \times \mathbf{Z}_2$ symmetry (30a)–(30c) of the problem and can therefore be regarded as a function $\tilde{\mathcal{H}}_{n,c}$ on the full symmetry reduced phase space $V_{n,c}^0$. In other words, $\mathcal{H}_{n,c}$ depends only on $\mathbf{Z}_2 \times \mathbf{Z}_2$ invariant polynomials π_1^2 (or w) and π_2 (see Appendix A.3). In order to define the function $\tilde{\mathcal{H}}_{n,c}$ on $V_{n,c}^0$ we express \mathcal{H}_{snf} (23a)–(23c) in terms of the invariants π_2 , π_1 , and π_4 , fix the value of π_4 to be c , and then change to the symmetry coordinate w in (31). In this way we find

$$\tilde{\mathcal{H}}_{n,c} = a\pi_2 + bw, \quad a = \alpha^2, \quad b = \frac{1}{2} - \alpha^2 - \alpha^4. \quad (33)$$

Here we have used the relations

$$x_1^2 + y_1^2 = \frac{1}{2}(\pi_1^2 + \pi_4^2), \quad x_1 y_1 = \frac{1}{4}(\pi_4^2 - \pi_1^2),$$

have rescaled time $t \rightarrow \frac{1}{2}t$, and have dropped the additive constant

$$\frac{1}{6}c^2(6\alpha^4 - 4\alpha^2 + 7) + \frac{1}{12}n^2(4\alpha^4 + 8\alpha^2 - 3) + \frac{1}{4}cnb.$$

We note that (to our order of the second normal form) this constant term contains all the dependence on the values of integrals n and c of the first and second normal forms. Even at the third order, the second normal form $\tilde{\mathcal{H}}_{n,c}$ remains linear in π_2 and w (see Appendix A.3).

3.3. Geometric analysis

We now analyse the geometry of the level sets of the second reduced normal form $\mathcal{H}_{n,c}$ on the second reduced phase space $P_{n,c}$ when $c = 0$, i.e., when $P_{n,c}$ is singular. It suffices to understand the h -level sets of $\tilde{\mathcal{H}}_{n,0}$ on the full symmetry reduced space $V_{n,0}^0$. There are two qualitatively different possibilities which are illustrated in Figs. 6 and 7. In these figures we also show the corresponding sets on the $\{\pi_3 = 0\}$ -projection of $P_{n,0}$. This latter representation

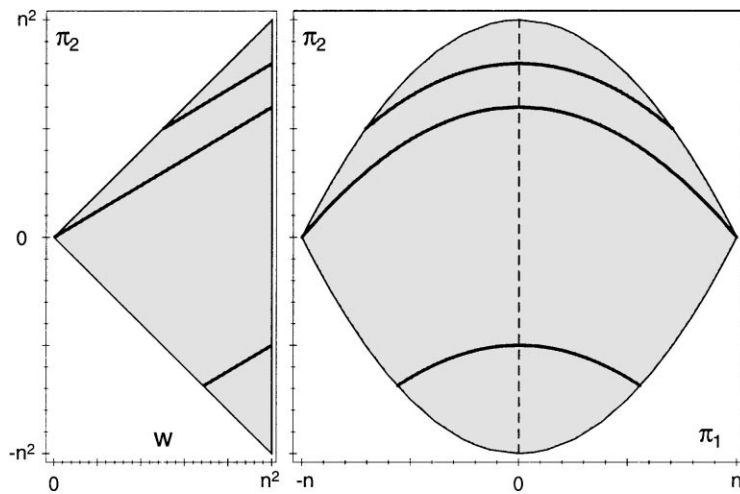


Fig. 7. Constant level sets of $\tilde{\mathcal{H}}_{n,0}$ on $V_{n,0}^0$ (left) and on $P_{n,0}^0$ (right) in the case when $|b/a| < 1$ (with monodromy). Corresponding levels on $V_{n,0}$ and $P_{n,0}$ are shown in Figs. 3 and 5.

was used in Refs. [25,26]. Furthermore, when $|b/a| < 1$, the same level sets can be seen in Figs. 3 and 5 on $P_{n,0}$ and $V_{n,0}$, respectively.

We now determine at what values of the parameter $\alpha \in [0, 1]$ the slope $|b/a|$ is less than 1. In other words, we want to have a system of level sets of the kind shown in Fig. 7 where the 0-level set of $\tilde{\mathcal{H}}_{n,0}$ is a closed interval one of whose end points is the singular point $(w, \pi_2) = (0, 0)$. Since $a = \alpha^2 > 0$, the condition that needs to be satisfied is $-a < b < a$. From (33), we see that the parameter $\alpha > 0$ must satisfy

$$-\alpha^2 < -\alpha^4 - \alpha^2 + \frac{1}{2} < \alpha^2.$$

The above inequalities become equalities when $\alpha^2 = \frac{\sqrt{2}}{2}$ and $\alpha^2 = \frac{\sqrt{6}}{2} - 1$. Hence $|b/a| < 1$ if and only if

$$\alpha^2 \in \mathcal{I} = \left(\frac{\sqrt{6}}{2} - 1, \frac{\sqrt{2}}{2} \right). \tag{34}$$

3.4. Reconstruction and monodromy

We now show how to reconstruct the geometry of the level sets of the second normal form on M_0 from the geometry of the level sets of the second reduced Hamiltonian on the second reduced phase space $P_{n,0}$. We will use the reduction map

$$\Pi : M_0 \subseteq S_{n/2}^2 \times S_{n/2}^2 \rightarrow P_{n,0} \subseteq \mathbf{R}^3 : (x, y) \rightarrow (\pi_1(x, y), \pi_2(x, y), \pi_3(x, y)), \tag{35}$$

whose fiber $\Pi^{-1}(p)$ over a point p in $P_{n,0}$ is a unique φ_t orbit on M_0 . If p is a nonsingular point of $P_{n,0}$, then $\Pi^{-1}(p)$ is a circle (i.e., a generic φ_t orbit); whereas if p is a singular point of $P_{n,0}$ then $\Pi^{-1}(p)$ is a point, which is fixed by the action φ_t .

We carry out our reconstruction only when $|b/a| < 1$. The treatment of the other case when $|b/a| > 1$ is analogous and is omitted. To follow the discussion please refer to Fig. 3 as well as Figs. 5 and 7 which illustrate the lift from $V_{n,0}^0$ to $P_{n,0}$. We begin by considering the case when the level set of $\mathcal{H}_{n,0}$ is a point p . If p is a nonsingular point of $P_{n,0}$ (with coordinates $\pi_1 = 0$ and $|\pi_2| = n$), then after reconstruction we obtain a periodic orbit $S^1 = \Pi^{-1}(p)$ of

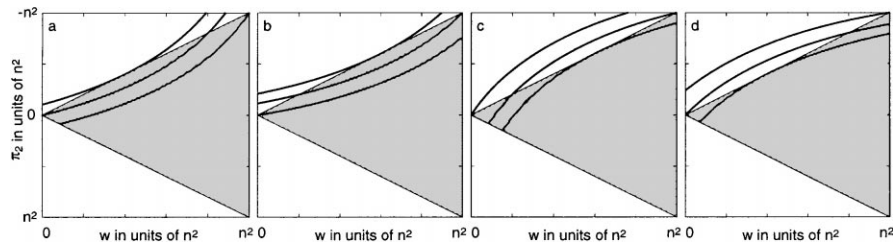


Fig. 8. Possible generic deformations of the constant level sets of \mathcal{H}_{snf} (33) when $a/b \approx 1$. All cases have an extra \mathbf{Z}_2 equivalent pair of relative equilibria. In the leftmost situation (a) the double pinched torus is decomposed into a \mathbf{Z}_2 equivalent pair of single pinched tori.

$X_{\mathcal{H}_1}$ on M_0 which is also a periodic orbit of $X_{\mathcal{H}_{\text{snf}}}$ since \mathcal{H}_{snf} and \mathcal{H}_1 Poisson commute. These periodic orbits are called relative equilibria of $X_{\mathcal{H}_{\text{snf}}}$. If p is a *singular* point of $P_{n,0}$, then after reconstruction we obtain an equilibrium point of $X_{\mathcal{H}_1}$ on M_0 which is also an equilibrium point of $X_{\mathcal{H}_{\text{snf}}}$.

We now look at the 0-level set of $\mathcal{H}_{n,0}$. This level set contains the two singular points p_0 and p_1 of $P_{n,0}$. If we remove these points, we obtain two curves \mathcal{C}_0 and \mathcal{C}_1 which consist of nonsingular points of $P_{n,0}$ and which are each topologically an open interval. Over each point on \mathcal{C}_i the fiber of the reduction map Π (35) is a circle. Since each \mathcal{C}_i is contractible in $P_{n,0} - \{p_0, p_1\}$ to a point, it follows that $\Pi^{-1}(\mathcal{C}_i)$ (the set of all points in M_0 which map by Π to points of \mathcal{C}_i) is diffeomorphic to a cylinder $\mathcal{C}_i \times S^1$. Thus, $\Pi^{-1}(\mathcal{C}_i \cup \{p_0, p_1\})$ is a cylinder with each of its ends pinched to a point. The reconstruction $\Pi^{-1}(\mathcal{H}_{n,0}^{-1}(0))$ in M_0 of the 0-level of $\mathcal{H}_{n,0}$ on $P_{n,0}$ is the union of two pinched cylinders with their end points identified two at a time to two distinct points. In other words, after reconstruction, the 0-level set of the second reduced Hamiltonian on the second reduced space is a doubly pinched 2-torus in M_0 (see Fig. 1, right). This doubly pinched 2-torus is the fiber over the (0,0) point in the range of the energy–momentum map \mathcal{EM} of the integrable system $(\mathcal{H}_{\text{snf}}, \mathcal{H}_1)$. Thus the energy–momentum map \mathcal{EM} has monodromy [12] when the values of α^2 lie in the interval \mathcal{I} (34).

3.5. Monodromy of the generic second normal form

The careful reader should have noticed that the reduced second normal form $\tilde{\mathcal{H}}_{\text{snf}}^{(1)}$ (33) truncated at order one (which corresponds to second order of the first normal form \mathcal{H}_{fnf}) is not generic. Indeed, when $|a/b| = 1$ the level sets of $\tilde{\mathcal{H}}_{\text{snf}}^{(1)}$ are parallel to one of the edges of $V_{n,0}^0$ (and thus the corresponding level set of $\mathcal{H}_{\text{snf}}^{(1)}$ coincides with part of $P_{n,0}^0$), see Figs. 6 and 7. In a generic situation the level sets of $\tilde{\mathcal{H}}_{\text{snf}}$ are slightly curved.

The two possible level sets of the generic $\tilde{\mathcal{H}}_{\text{snf}}$ are illustrated in Fig. 8. The level sets near the edge $|\pi_2| = w$ of $V_{n,0}^0$ can either curve “inward” as in Fig. 8(a) and (b) or “outward” as in Fig. 8(c) or (d). To find which situation occurs in our problem, the *fourth* order of the first normal form \mathcal{H}_{fnf} (which corresponds to the third order $\mathcal{H}_{\text{snf}}^{(3)}$ of the second normal form) should be computed (see Appendix A.3). The terms $a'\pi_1^2\pi_2$, $b'\pi_1^4$ and $c'\pi_2^2$ in $\mathcal{H}_{\text{snf}}^{(3)}$ ensure that the level sets of $\tilde{\mathcal{H}}_{\text{snf}}^{(3)}$ are curved. According to our fourth-order analysis [41] both the “inward” and “outward” cases occur.

When $|a/b| \approx 1$ and $c = 0$ the generic $\tilde{\mathcal{H}}_{\text{snf}}^{(3)}$ has an extra pair of \mathbf{Z}^2 -equivalent relative equilibria. These correspond to a point of tangency of a level set of $\tilde{\mathcal{H}}_{\text{snf}}^{(3)}$ with one of the edges of $V_{n,0}^0$. As a/b changes the point of tangency moves quickly to one of the endpoints of the edge and disappears. There are two bifurcations involved in this process. At the first, the \mathbf{Z}^2 -equivalent pair of relative equilibria appears from the singular points $\pi_2 = 0$, $V_1 = \pm n$ (i.e., $\pi_2 = w = 0$) of the second reduced phase space $P_{n,0}$. At the second, this pair collapses to one of the \mathbf{Z}_2 -symmetric relative equilibria $w = |\pi_2| = n$. The first bifurcation is a $\mathbf{S}^1 \times \mathbf{Z}^2$ -symmetric Hamiltonian Hopf bifurcation [41], whereas the second is a pitchfork bifurcation.

When $|a/b| \approx 1$ and $c = 0$ (near the limits of the monodromy interval \mathcal{I} (34)) the topology of the level sets of the generic \mathcal{H}_{snf} (which lie near $|\pi_2| = w$) can be quite complicated. In particular, Fig. 8(a) shows how the zero-level set which corresponds to the doubly pinched 2-torus in M_0 , see Fig. 7, splits into two singly pinched 2-tori. Even though the topology of the zero-level set of $\tilde{\mathcal{H}}_{\text{snf}}^{(3)}$ is different from the topology of the zero-level set of $\tilde{\mathcal{H}}_{\text{snf}}^{(1)}$, the monodromy does *not* change because $\tilde{\mathcal{H}}_{\text{snf}}^{(1)}$ and $\tilde{\mathcal{H}}_{\text{snf}}^{(3)}$ on M_0 are smoothly homotopic and monodromy is a homotopy invariant. Consequently, our geometric analysis of the nongeneric second normal form $\tilde{\mathcal{H}}_{\text{snf}}^{(1)}$ is adequate for determining the monodromy.

4. Quantum monodromy

Traditionally, manifestations of monodromy in quantum systems have been analysed using the quantum analogue of the energy–momentum map [13–16]. The EBK quantization conditions for an integrable system select regular sequences of invariant tori which correspond to quantum energy levels. The global structure of energy levels of the quantum analogue of an integrable system with monodromy is quite particular and provides a very clear manifestation of monodromy [10,11,13,14]. Locally, the energy levels (and the corresponding tori) form a regular lattice of points in the range of energy–momentum map \mathcal{EM} and can be labelled by the values of quantized actions. However, if monodromy is present, the structure of this lattice in the vicinity of the image of the pinched torus makes any global labelling impossible.

4.1. Quantum analogue of the second normal form

The technique to construct the quantum analogue of the normalized Kepler Hamiltonian (of the first reduced Hamiltonian \mathcal{H}_{inf} on $S_{n/2}^2 \times S_{n/2}^2$) is well known, see [42–44].⁶ To construct the quantum analogue $\hat{\mathcal{H}}_{\text{snf}}$ of the second reduced Hamiltonian $\mathcal{H}_{\text{snf}}(\pi_1^2, \pi_2)$ (33) we represent the latter in terms of components of the 3-vectors x and y in (16a) and (16b) and then replace x and y with their quantum analogues. The Poisson algebra (18) is the algebra $\text{su}(2) \times \text{su}(2)$ of two angular momenta. It corresponds to the algebra of quantum angular momentum operators

$$[\hat{x}_a, \hat{x}_b] = i\varepsilon_{abc}\hat{x}_c, \quad [\hat{y}_a, \hat{y}_b] = i\varepsilon_{abc}\hat{y}_c, \quad [\hat{x}_a, \hat{y}_b] = 0, \quad (36)$$

where $\{abc\} = \{123\}$ and $[A, B] = AB - BA$. The Casimirs of this algebra are x^2 and y^2 in (17). They are integrals of the second normal form. Hence in quantum mechanics $[\hat{\mathcal{H}}_{\text{snf}}, \hat{x}^2] = [\hat{\mathcal{H}}_{\text{snf}}, \hat{y}^2] = 0$. The standard angular momentum quantization gives

$$\hat{x}^2 = \hat{y}^2 = j(j+1), \quad j = 0, \frac{1}{2}, 1, \frac{3}{2}, \dots \quad (37a)$$

Here j labels the natural $\text{su}(2)$ representation of dimension $2j+1$. The $(2j+1)^2$ quantum states with quantum number j form an n shell of the perturbed hydrogen atom system with the number of states, when expressed in terms of the principal quantum number

$$n = 2\langle \hat{x}^2 + \hat{y}^2 \rangle = \langle \hat{\mathbf{T}}^2 + \hat{\mathbf{V}}^2 \rangle = 1, 2, 3, \dots, \quad (37b)$$

being n^2 . Consequently,

$$j = \frac{1}{2}(n-1). \quad (38a)$$

It follows from (17) that

$$\hat{x}^2 = \hat{y}^2 = j(j+1) = \frac{1}{4}(n^2 - 1) = \frac{1}{4}\langle \hat{N}^2 \rangle \quad (38b)$$

⁶ In [42] authors used $b \approx \alpha^{-2} - 2\alpha^2 - 2$ as a field parameter.

and that the classical value of the Kepler integral N is

$$n_{\text{cl}} = \sqrt{\langle \hat{N}^2 \rangle} = \sqrt{n^2 - 1}. \quad (38\text{c})$$

At the same time the quantum number m of the integral of motion $T_1 = x_1 + y_1$ (the projection of the angular momentum T on the axis of the dynamical \mathbf{S}^1 symmetry) takes all integer values in the interval

$$m = \langle \hat{T}_1 \rangle = m_x + m_y = -2j, \dots, 2j = -(n-1), \dots, n-1. \quad (39)$$

(Here m_x and m_y correspond to the projection operators \hat{x}_1 and \hat{y}_1 , respectively.) The classical value c of T_1 equals m . To find the quantized energies we solve a simple matrix problem for each value of m at a fixed value of quantum number n . In the standard spherical harmonic basis $\psi_{j,m_x,m_y} = Y_{j,m_x} Y_{j,m_y}$ with $m_x + m_y = m$, we obtain a Hermitian matrix of dimension $2j + 1 - m = n - m$ which can be further reduced if the $\mathbf{Z}_2 \times \mathbf{Z}_2$ symmetry is taken into account.

The quantum analogue of the Hamiltonian

$$\mathcal{H}_{\text{snf}} = a\pi_2 - b\pi_1^2 \quad (40\text{a})$$

in (33) is the operator

$$\hat{\mathcal{H}}_{\text{snf}} = 2a(\hat{x}^+ \hat{y}^- + \hat{x}^- \hat{y}^+) - b(\hat{x}_1 - \hat{y}_1)^2, \quad (40\text{b})$$

where $\hat{x}^\pm = \hat{x}_2 \pm i\hat{x}_3$ and $\hat{y}^\pm = \hat{y}_2 \pm i\hat{y}_3$ are creation–annihilation operators. Using standard formulae [45,46], we find

$$\hat{\mathcal{H}}_{\text{snf}} \psi_{j,m_x,m_y} = 2a(t_{m_x}^+ t_{m_y}^- \psi_{j,m_x+1,m_y-1} + t_{m_x}^- t_{m_y}^+ \psi_{j,m_x-1,m_y+1}) - b(m_x - m_y)^2 \psi_{j,m_x,m_y}, \quad (41)$$

where coefficients $(t_k^\pm = ((j \mp k)(j \pm k + 1))^{1/2})$. It can be seen that the value $m_x + m_y = m = c$ is preserved, the matrix of $\hat{\mathcal{H}}_{\text{snf}}$ is tridiagonal,⁷ and our calculation is essentially a reproduction of [42].

4.2. Analysis of quantum energy–momentum map

Results of our computation for $n = 11$ and the corresponding classical value of $n_{\text{cl}} = \sqrt{120}$ are shown in Fig. 9. Black dots in this figure show the eigenvalues of the matrix of $\hat{\mathcal{H}}_{\text{snf}}$ in the basis with $n = 11$ and $m = -10, \dots, 10$, bold lines represent stationary points of $\mathcal{H}_{n,0}$ on $P_{n,0}$ with $n_{\text{cl}} = \sqrt{120}$. These lines limit the range of the classical energy–momentum map \mathcal{EM} . The case with monodromy ($a/b = 0.4$ and $\alpha^2 \sim 0.295$) is shown on the left of Fig. 9. We compare and analyse quantum energy–momentum map for $n = 11$ and classical \mathcal{EM} for $n_{\text{cl}} = \sqrt{120}$.

It can be seen that quantum energies form a 2-lattice in the range of \mathcal{EM} . In the presence of monodromy this lattice has a *point defect* located at the value of \mathcal{EM} corresponding to the pinched torus. The type of the defect is related to the number and type of the pinch points. To visualize this defect we can define an elementary cell of the lattice and transport it along a path which lies entirely in the domain of regular values of \mathcal{EM} and goes around

⁷ Thus in the case $n = 4$ the $c = m_x + m_y = 0$ subspace is spanned by four functions $\psi_{j,m,-m}$ with $j = \frac{3}{2}$ and $m = -\frac{3}{2}, -\frac{1}{2}, \frac{1}{2}, \frac{3}{2}$. The matrix representation of $\hat{\mathcal{H}}_{\text{snf}}$ on this subspace is

$$\begin{pmatrix} -9b & 6a & & & \\ 6a & -b & 8a & & \\ & 8a & -b & 6a & \\ & & 6a & -9b & \end{pmatrix}.$$

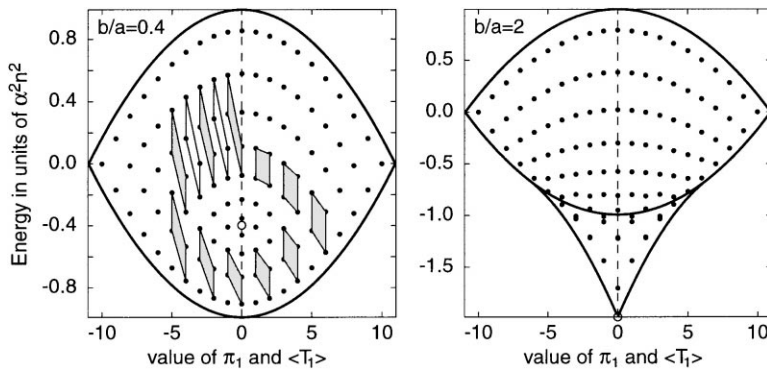


Fig. 9. Quantum and classical energy–momentum map for quantum number $n = 11$ and classical value $n_{cl} = \sqrt{120}$. In the case with monodromy (left) the position of the pinched torus is marked by a white circle and the deformation of the local lattice is shown by a sequence of shaded quadrilaterals.

the defect (Fig. 9, left). We can easily follow the evolution of this cell because each small step to a neighbouring cell is unambiguous. However, after making a tour our final cell does *not* match the original cell! The accumulated deformation is described by the matrix

$$\begin{pmatrix} 1 & 2 \\ 0 & 1 \end{pmatrix},$$

where 2 corresponds to the number of pinch points of the singular fiber of the energy–momentum map [40]. Thus the lattice in Fig. 9 (left) cannot be labelled globally by two quantum numbers.

For comparison, we show on the right of Fig. 9 the results of the same calculation for $\alpha^2 \sim 0.158$. In this case the value of α^2 lies outside the monodromy interval \mathcal{I} and is close to the Stark limit where $\alpha = 0$. The corresponding energy level spectrum is quite similar to that in the quadratic Zeeman effect [47–49]. Two distinct regions in the range of \mathcal{EM} are clearly separated by the energy of an unstable \mathbf{Z}_2 symmetric stationary point of $\mathcal{H}_{n,c}$. In the lower region the quantum lattice corresponds to that of a rotator with angular momentum quantum number $J = n, n - 1, \dots$. The upper region corresponds to the double well 2-oscillator. Over each of the regions (except, perhaps, for a few levels near their common boundary) there is a straightforward unambiguous labelling with two quantum numbers. From (33) we can see that $b/a \geq -\frac{3}{2}$, and that to the order used in our second reduced Hamiltonian $\mathcal{H}_{n,c}$ the structure at $b/a < -1$ is qualitatively the same as in Fig. 9, right, with the energy axis flipped.

The whole parametric family of \mathcal{EM} can be easily imagined if we note that in the Zeeman limit at $\alpha = 0$ the Hamiltonian $\mathcal{H}_{n,0}$ has an absolute minimum at the singular points p_1 and p_2 of $P_{n,0}$. As the value of α^2 increases, the value $\mathcal{H}_{n,0}(p_1) = \mathcal{H}_{n,0}(p_2)$ also increases. Thus the double-well region shrinks. When $\alpha^2 = \frac{1}{2}\sqrt{6} - 1$, $\mathcal{H}_{n,0}(p_1)$ enters the (upper) rotator region. Here the points p_1 and p_2 become hyperbolic relative equilibria and their stable and unstable manifolds connect. After reconstruction they form a double pinched torus in M_0 . In this region the angular momentum quantization rule breaks down (Fig. 9, left). As $\mathcal{H}_{n,0}(p_1)$ continues to increase, it becomes an absolute maximum when $\alpha^2 > \sqrt{2}/2$ (Fig. 9, right).

5. Comments on previous work on the crossed fields problem

Our methods, especially the analysis based on the second normal form can be used for a complete qualitative study of the crossed fields system in all possible dynamical regimes. In particular, all invariant subsets (regular tori, periodic orbits, etc.) and their bifurcations can be fully characterized and systematized. Many other perturbed

Kepler systems can be studied in a similar way. As our purpose was to focus on monodromy, we have addressed such a complete analysis but very briefly. Below we give more details on the applications of our methods and interpret previously obtained results. This section is mostly destined for atomic physicists who are aware of the vast literature on the atoms-in-fields problem and want to place properly our present work. At the same time, though far from being comprehensive, it can help mathematicians get a feeling of what has gone on in this particular field of atomic physics during the past 20 years.

5.1. Parameterization schemes

When comparing classical and quantum results, we should be well aware of the difficulty presented by the two different parameterization schemes (cf. Sections IIE and IVB1 in [24]). In brief, we tend to use energy-scaled field strengths in classical mechanics and n scaled field strengths in quantum mechanics. In other words, in the classical problem we work on the same energy level set of (1), whereas in the quantum problem we compute energies of the states within the same n -shell. Formally, the energy of our system can be found as follows. Remember that for the initial KS Hamiltonian in (6) the energy is $4/\omega$. Similar relation between the value of the Hamiltonian function and ω holds for the first and second normal form and should be used to find the value of ω (and energy). If we take all our rescalings properly into account and include all constant terms, this relation for the second normal form $\tilde{\mathcal{H}}_{\text{snf}}$ in (33) is

$$\begin{aligned} \mathcal{H}_{\text{snf}} &= \frac{c}{n} - \frac{1}{4}\varepsilon n \left[a \frac{\pi_2}{n^2} - b \frac{\pi_1^2}{n^2} + \left(\frac{17}{6} - \frac{7}{3}a + a^2 \right) \frac{c^2}{n^2} + \frac{17}{18} - \frac{19}{9}a - \frac{1}{3}a^2 \right] + (\varepsilon n)^2 \frac{c}{n} \frac{\mathcal{F}(\pi_2, \pi_1^2, c^2; a)}{n^2} + \dots \\ &= \frac{c}{n} - \frac{1}{4}(\varepsilon n) \frac{h}{n^2} + (\varepsilon n)^2 \frac{c}{n} \frac{\mathcal{F}}{n^2} + \dots = -\frac{2}{\varepsilon n} + \frac{2S}{(\varepsilon n)^2}, \end{aligned} \quad (42)$$

where \mathcal{F} comes from the third order term obtained in Ref. [27], h is the value of $\tilde{\mathcal{H}}_{\text{snf}}$ in (33) plus a constant, and $\varepsilon = \frac{1}{2}S\omega$ [24]. (Note that $\pi_1, \pi_4 = c$, and π_2 are scaled according to the degree in T and V , and since $T^2 + V^2 = n^2$, all dependence on the Keplerian action n is now absorbed in the formal series parameter (εn) .) Eq. (42) leads to a formal power series in εn

$$S = (\varepsilon n) + \frac{1}{2}(\varepsilon n)^2 \frac{c}{n} - \frac{1}{8}(\varepsilon n)^3 \frac{h}{n^2} + \dots \quad (43a)$$

Inverting (43a) gives

$$\varepsilon = \frac{S}{n} - \frac{1}{2}c \frac{S^2}{n^2} + \left(\frac{1}{2}c^2 + \frac{1}{8}h \right) \frac{S^3}{n^3} - c \left(\frac{5}{8}c^2 + \frac{5}{16}h + \mathcal{F} \right) \frac{S^4}{n^4} + \dots, \quad (43b)$$

and consequently,

$$\frac{2\sqrt{-2E}}{C} = \omega = \frac{2}{n} \left[1 - \frac{1}{2}c \frac{S}{n} + \left(\frac{1}{2}c^2 + \frac{1}{8}h \right) \frac{S^2}{n^2} + \dots \right] \quad (43c)$$

(recall the discussion in Section 2.1). It follows that the energy is

$$E = -\frac{C^2}{2n^2} \left[1 - c \frac{S}{n} + \frac{1}{4}(5c^2 + h) \frac{S^2}{n^2} - \frac{1}{4}c(7c^2 + 3h + 8\mathcal{F}) \frac{S^3}{n^3} + \dots \right]. \quad (43d)$$

In (43d) the unperturbed hydrogen atom energy is factored out. The smallness parameter S [24] is a uniform field strength parameter. Its n -shell definition can be obtained from the energy-scaled formulae in Section 3.1, if the KS frequency ω is replaced by $2/n$ so that

$$S \rightarrow n \left[\left(\frac{Gn^2}{C^2} \right)^2 + \left(\frac{3Fn^3}{C^6} \right)^2 \right]^{1/2}. \quad (44)$$

The two definitions are equivalent in the unperturbed Kepler problem. In our case a simple replacement (44) gives the principal order terms and is qualitatively correct. Accurate calculation requires the reparameterization of the first normal form \mathcal{H}_{fnf} using the value of n instead of ω in the definition of scaled field strengths.

5.2. First normalization and relative equilibria

In the early analysis of the hydrogen atom in magnetic field (quadratic Zeeman effect) Keplerian symmetry was averaged along the corresponding \mathbf{S}^1 orbits [47,48,50].⁸ Later Levi–Civita regularization was implemented, the resulting two-dimensional Hamiltonian was normalized to high orders, and quantized [43,44]. Full regularization of the three dimensional system using Kustaanheimo–Stiefel method was introduced in Refs. [17–22]. Subsequently, any hydrogen atom-in-fields system could be transformed in a regular perturbation of a 1:1:1 oscillator and normalized straightforwardly using standard Lie series technique [51–53] to any required order. (As an alternative, Moser’s regularization in [25,26] and Delaunay normalization in [54], both used to the first order, can be mentioned.)

The normal form \mathcal{H}_{fnf} of the crossed fields problem was reported in [38] and later in [30–32]. However, in subsequent work [35–37] the authors turned to the analysis of the second reduced problem. As in [33,34,38] the reorientation $(L, K) \rightarrow (T, V)$ and the use of T_1 as the “third” approximate integral was the starting point of this analysis (see Section 5.5). In that way the problem was made similar to the familiar cases with spatial \mathbf{S}^1 symmetry (Zeeman effect and parallel fields, see Section 5.3) and was analysed for each fixed value c of T_1 separately. The authors of [30–32] considered the case $|c| \neq n$ which they fully analysed only for $c \neq 0$. (They did not consider the geometry of their system, and in particular the relative equilibria and the associated singularity of $P_{n,c=0}$.) On the other hand, relative equilibria with $c = \pm n$ ($P_{n,c=\pm n}$ is a point) and with $c = 0$ (singular point of $P_{n,c=0}$) were studied in Ref. [33,34].⁹

A comprehensive study of these relative equilibria was presented in [24] where the position of the equilibria on $\mathbf{S}^2 \times \mathbf{S}^2$, action and period of the corresponding periodic orbits, as well as reconstruction of these orbits in the physical space of the Kepler problem were obtained *entirely* on the basis of the first normalized system. The techniques used in [24], namely invariant theory, full study of the $\mathbf{S}^2 \times \mathbf{S}^2$ geometry, analysis of the symmetry group action, and Morse theory, make this work a direct predecessor of and a complement to our present study. Since [24] dealt exclusively with four basic relative equilibria, no second normalization was required.

At the same time it should be remarked that *all* results of [24] can be obtained straightforwardly from the second normal form \mathcal{H}_{snf} . Thus to find the action integral along the periodic orbit with $|\pi_1| = n$ in the KS space (\mathcal{T}_s orbit in Table 2 of [24]), we substitute the coordinates $(\pi_1, \pi_2) = (\pm n, 0)$ of the singular point on $P_{n,c=0}$ in (42). We obtain the formal series in εn

$$S = \varepsilon n + \frac{1}{36}(\varepsilon n)^3(1-a)(3a-2) + O((\varepsilon n)^5), \quad (45a)$$

whose inverse is

$$\varepsilon n = S - \frac{1}{36}S^3(1-a)(3a-2) + O(S^5). \quad (45b)$$

⁸ In the notation of these authors ([50], Table I), angle ϕ_3 is the coordinate along the \mathbf{S}^1 orbit of the Keplerian symmetry, $I_3 \propto n$ is the corresponding action; they use $I_2^2 = L^2$ which corresponds to $\frac{1}{2}(\pi_2^2 - \pi_1^2 + n^2 + c^2)$.

⁹ The “elementary Kepler ellipses” or periodic orbits studied by these authors are four relative equilibria of the first normal form. The periodic orbit S_\perp (they do not distinguish two symmetry equivalent S_\perp orbits) has stabilizer σ_3 in (30a)–(30c) and corresponds to the two singular points of $P_{n,c=0}$ (with $\pi_2 = \pi_3 = 0$ and $\pi_1 = \pm n$). The periodic orbits S_- (“downhill”) and S_+ (“uphill”) are $\mathbf{Z}_2 \times \mathbf{Z}_2$ -symmetric relative equilibria, they correspond to $P_{n,c=\pm n}$ (points $\pi_1 = \pi_2 = \pi_3 = 0$ and $\pi_4 = \pm n$). See [24], Footnote 4, and Section 5.2.

Using the relation $\varepsilon = \frac{1}{2}S\omega$ [24] we find the action along the orbit

$$\frac{1}{2\pi} \oint p dq = n = \frac{2}{\omega} \left[1 - \frac{1}{36} S^2 \beta^2 (3\alpha^2 - 2) + O(S^4) \right]. \quad (45c)$$

To reconstruct the orbit in the KS space we should first find the position of the equilibrium point on $\mathbf{S}^2 \times \mathbf{S}^2$ using the inverse second normal form transformation and then proceed as in Ref. [24].

Thus we conclude that the first normalized system is an intermediate stage in the analysis, which can be omitted if the geometry of the two step reduction is given. Then the complete qualitative understanding of the dynamics of our system can be obtained when all individual second normalized systems (with phase spaces $P_{n,c}$ and Hamiltonians $\mathcal{H}_{n,c}$) are studied as one family.

5.3. Systems with additional \mathbf{S}^1 -symmetry

The methods of geometrical and dynamical analysis presented in our paper apply *equally* to any perturbed Kepler problem with an additional \mathbf{S}^1 symmetry as long as this additional symmetry commutes with the \mathbf{S}^1 symmetry of the first reduction and induces the same diagonal action on the first reduced phase space $\mathbf{S}^2 \times \mathbf{S}^2$. The additional \mathbf{S}^1 symmetry itself can be exact or, as in our case, an approximate dynamical symmetry “imposed” by the second normalization. The most obvious and widely studied case of such symmetry (complete bibliography on the subject is very large, see [17–23,28,29,43,44,47–49] and other work cited there) is an axially symmetric system such as hydrogen atom perturbed by only one field (magnetic or electric) or by two parallel fields. In this case, the \mathbf{S}^1 action on the 3-vectors K and L in the initial physical space of the Kepler problem is a simultaneous rotation about the symmetry axis, or the field(s) axis (chosen as axis Q_1 here or z elsewhere)

$$(K, L) \rightarrow (R_\phi K, R_\phi L), \quad R_\phi = \begin{pmatrix} 1 & 0 & 0 \\ 0 & \cos \phi & \sin \phi \\ 0 & -\sin \phi & \cos \phi \end{pmatrix}.$$

Such action is equivalent (conjugate) to (21). Consequently, there is a simple correspondence between our second normalized system with integrals n and $T_1 = \pi_4 = c$ and a first normalized axially symmetric system with integrals n and $L_1 = m$, the projection of the angular momentum. In particular, to obtain invariant polynomials for the latter system (see Appendix A.1) we should take (25a)–(25f) and simply substitute (L, K) for (T, V) .

Furthermore, one should note that second and first normalizations use the *same* smallness parameter ε and in this regard second normalized system and its \mathbf{S}^1 symmetry come at no additional cost — they remain valid as long as the first normal form does. Since first normalization is common to all perturbed Kepler systems we consider, it appears that to the order of this approximation, the \mathbf{S}^1 symmetry of our system and the strict \mathbf{S}^1 symmetry mentioned above are equivalent.

5.3.1. Reduction of finite symmetries

The finite symmetries which remain after the additional \mathbf{S}^1 symmetry is removed are system specific [56].¹⁰ The parallel fields system [23] has only one reversing symmetry \mathbf{Z}_2 which acts on invariants of the second reduced system in the same way as σ_3 acts on (π_1, π_2, π_3) in (30c). The residual finite symmetry in the case of the Zeeman effect (only magnetic field) and Stark effect (only electric field) is $\mathbf{Z}_2 \times \mathbf{Z}_2$ with action (30a)–(30c). Within our framework these are two particular cases ($a = \alpha = 1$ and $b = -\frac{3}{2}$) and ($\alpha = 0$), respectively. It should be noted that

¹⁰ The initial unpublished version of this work is dated 1995. As in [23] and Appendix A.1 the authors use n -scaled invariants. Due to slightly different choice of invariants (ξ vs π_2) their orbifold has the shape of a smoothed tetrahedron, see Fig. 4 in [23], where such choice is dictated by the concrete Hamiltonian linear in ξ and π_1 .

the symmetry of the corresponding original system is very different. Thus the pure Stark problem is symmetric with regard to momentum reversal $(q, p) \rightarrow (q, -p)$ whose *image* in the ambient 3-space with coordinates (π_1, π_2, π_3) is (30a) (in this limit $\pi_4 = K_2$ and $\pi_1 = L_2$).

5.3.2. Orbifold method

A comprehensive analysis of symmetries of different possible perturbations of the Kepler problem (e.g. of the hydrogen atom) was given by Žhilinskii and Michel in Ref. [56]. After reducing the Keplerian symmetry $O(4)$ (n -shell approximation) these authors consider various symmetry group actions on the first reduced phase space $\mathbf{S}^2 \times \mathbf{S}^2$. Using only group theory and invariant polynomials they reduce symmetries and represent the respective reduced Hamiltonian functions on the space of orbits or the *orbifold* of the symmetry group action. We briefly apply the approach of [56] to our concrete system.

In the presence of the additional \mathbf{S}^1 symmetry the space of orbits or “orbifold” \mathcal{O} is a three-dimensional algebraic variety on which we can define and analyse our Hamiltonian \mathcal{H}_{snf} . To construct \mathcal{O} we note that each orbit of the \mathbf{S}^1 action on $\mathbf{S}^2 \times \mathbf{S}^2$ can be labelled by the values of four invariants π_1, π_2, π_3 , and π_4 (which generate the ring of all \mathbf{S}^1 invariant polynomials) subject to the restriction (29a), where $\pi_4 = c$. From this restriction we see immediately that labelling of these orbits requires the values of only *three* invariants, such as π_1, π_2 , and π_4 , while for the fourth invariant π_3 only the sign should be given. It follows that \mathcal{O} can be embedded in Euclidean 3-space with coordinates $\{\pi_1, \pi_2, \pi_4\}$. The $\pi_3 > 0$ and $\pi_3 < 0$ points of \mathcal{O} form two balls whose closure is the surface $\{\pi_3 = 0\}$, which using (29a) is defined by

$$\pi_2^2 - [(n - \pi_4)^2 - \pi_1^2][(n + \pi_4)^2 - \pi_1^2] = 0. \tag{46}$$

In coordinates $\{\pi_1, \pi_2, \pi_4\}$ this surface resembles a square pillow (see Fig. 10, left). It is a 2-sphere with four singular points, the fixed points of the \mathbf{S}^1 action, where $\pi_2 = \pi_3 = 0$ and $\pi_1 = \pm n$ or $\pi_4 = \pm n$. The whole \mathcal{O} is a 3-sphere with four singular points. Every point of \mathcal{O} except these four lifts to an \mathbf{S}^1 on $\mathbf{S}^2 \times \mathbf{S}^2$. The four points are relative equilibria of the first reduced problem, they lift to four equilibrium points on $\mathbf{S}^2 \times \mathbf{S}^2$.

In the presence of an additional \mathbf{Z}_2 symmetry which sends $\pi_3 \rightarrow -\pi_3$ (typically a reversing symmetry such as σ_3 in (30a)–(30c)), the sign of π_3 is not required. The two balls in the previous construction are identified. The orbifold \mathcal{O} has three kinds of points which lift either to one or two circles, or to a point on $\mathbf{S}^2 \times \mathbf{S}^2$. This orbifold

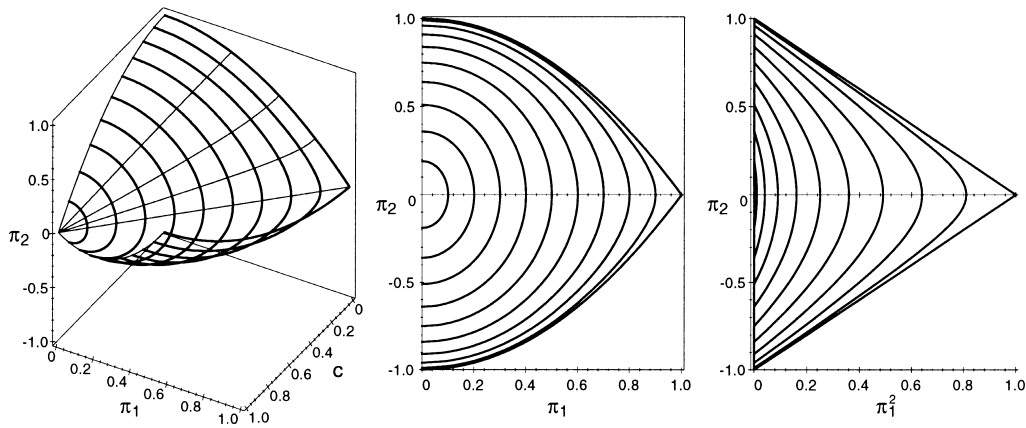


Fig. 10. Orbit space of the $\mathbf{S}^1 \times \mathbf{Z}_2$ action on $\mathbf{S}^2 \times \mathbf{S}^2$ for $c \geq 0$ and $\pi_1 > 0$. Bold line sections with constant $T_1 = \pi_4 = c, n \geq c \geq 0$, show images of second reduced phase spaces, $P_{n,c} \cap \{\pi_3 = 0\}$ (left). Projection of the orbit space on the $\{c = 0\}$ plane (centre). Projection of the orbit space of $\mathbf{S}^1 \wedge \mathbf{Z}_2 \times \mathbf{Z}_2$ (right). Coordinates π_1, c , and π_2 are in units of n, n and n^2 , respectively.

is constructed in Section III and Appendix A.3 of Ref. [56] and is used in Ref. [23]. The constant $\pi_4 = c$ sections of \mathcal{O} are images of reduced phase spaces $P_{n,c}$. We can fold \mathcal{O} once more in order to fully reduce $\mathbf{Z}_2 \times \mathbf{Z}_2$ (see Fig. 10, right, and compare to Figs. 6 and 7).

Our Hamiltonian itself can be expressed as a function of (π_1, π_2, π_4) .¹¹ Considering the topology of constant level sets of $\mathcal{H}_{\text{snf}}(\pi_1, \pi_2, \pi_4)$ defined on \mathcal{O} we can now analyse all reduced Hamiltonians $\mathcal{H}_{n,c}$ at once, see e.g. [11,23,56]. In this way we can, to some extent, compensate for the necessity to consider individual second reduced phase spaces $P_{n,c}$ which, however, remain indispensable for the study of the dynamics of the second reduced system.

5.3.3. Dynamics on the second reduced phase space

All systems with additional \mathbf{S}^1 symmetry described above will have the *same* second reduced phase space $P_{n,c}$. The dynamics of these systems can be described using the *same* Poisson algebra of invariants π_1, π_2 , and π_3 restricted to $P_{n,c}$, i.e., the Poisson structure of the second reduced system. This structure can be obtained in a straightforward way from definitions (25a)–(25f) and the Poisson structure on $\mathbf{S}^2 \times \mathbf{S}^2$ in (18), namely

$$\{\pi_1, \pi_2\} = 2\pi_3, \quad \{\pi_3, \pi_1\} = 2\pi_2, \quad \{\pi_2, \pi_3\} = 4\pi_1(n^2 + c^2 - \pi_1^2). \quad (47)$$

Furthermore, the function

$$\psi_{n,c}(\pi_1, \pi_2, \pi_3) = \pi_2^2 + \pi_3^2 - X_{n,c}^2(\pi_1^2) \quad (48a)$$

with

$$X_{n,c}^2(\pi_1^2) = (n - c - \pi_1)(n - c + \pi_1)(n + c - \pi_1)(n + c + \pi_1) \geq 0, \quad (48b)$$

whose 0-level defines the second reduced phase space $P_{n,c}$ in (29a), is a Casimir of the algebra (47). Using $\psi_{n,c}$ we can rewrite (47) as

$$\{\pi_i, \pi_j\} = \epsilon_{ijk} \frac{\partial \psi_{n,c}}{\partial \pi_k}, \quad (49)$$

and generate equations of motion as follows:

$$\dot{\pi}_i = \sum \frac{\partial \mathcal{H}_{\text{snf}}}{\partial \pi_j} \{\pi_i, \pi_j\} = \sum \epsilon_{ijk} \frac{\partial \mathcal{H}_{\text{snf}}}{\partial \pi_j} \frac{\partial \psi_{n,c}}{\partial \pi_k}. \quad (50)$$

Thus for the second normal form

$$\mathcal{H}_{\text{snf}} = a\pi_2 - b\pi_1^2 = h, \quad (51)$$

we obtain

$$\frac{d^2 \pi_1^2}{dt^2} = \{\{\pi_1^2, \mathcal{H}_{\text{snf}}\}, \mathcal{H}_{\text{snf}}\} = 8[3(a^2 - b^2)\pi_1^4 - 4(bh + a^2(n^2 + c^2))\pi_1^2 - h^2 + a^2(c^2 + n^2)^2], \quad (52)$$

where we have used $\mathcal{H}_{\text{snf}} = h$ and $\psi_{n,c} = 0$ to replace π_2 and π_3 . In terms of the new variable

$$\wp = 4(a^2 - b^2)\pi_1^2 - \frac{8}{3}(bh + a^2(n^2 + c^2)), \quad (53a)$$

¹¹ In Section 5.3.2, we decomposed the generators of the ring of \mathbf{S}^1 invariant polynomials into two groups, $\{\pi_1, \pi_2, \pi_4\}$ and $\{\pi_3\}$, called principal (or main) and auxiliary invariants. Such decomposition is known as integrity basis [62], homogeneous system of parameters [63], or Hironaka decomposition [64]. It is generally possible for Cohen–Macaulay rings. Main invariants define the same set of coordinates on *all* maps of \mathcal{O} while auxiliary invariant(s) distinguish different maps. Only degree 0 and 1 of auxiliary invariant(s) is necessary to express any polynomial in the ring. In the case of the full $\mathbf{S}^1 \wedge (\mathbf{Z}_2 \times \mathbf{Z}_2)$ symmetry the ring is freely generated by π_1^2, π_2 , and π_4 ; there are no auxiliary polynomials.

this equation reads

$$\ddot{\wp} = 6\wp^2 - \frac{1}{2}g_2. \tag{53b}$$

Its solution is the Weierstrass' function $\wp(t; g_2, g_3)$ [57].

5.4. Attempts to use a second reduced space in perturbed Kepler systems with \mathbf{S}^1 symmetry: the asymmetric top analogy

The angular momentum or asymmetric top interpretation of the perturbed hydrogen atom with axial (\mathbf{S}^1) symmetry, and in particular of the quadratic Zeeman effect (QZE) with integral $L_1 = m$ was introduced in 1990–1991 in Refs. [18–21,28,29], where the second reduced Hamiltonian was represented on a 2-sphere. (Note that earlier perturbation theory studies, such as [50], used “action–angle” variables, i.e., cylindrical coordinates, for their reduced Hamiltonian.) This approach has been used extensively in Refs. [22,54,55]. We saw in Section 3.2.1 that the second reduced space $P_{n,c}$ is *not always* diffeomorphic to a 2-sphere and therefore, such angular momentum analogy calls for comment. In essence, the \mathbf{S}^2 map used by these authors is *singular* for $m = 0$ (i.e., $c = 0$). It is important to understand the consequences of such singularity. To show once more that the axially symmetric perturbation of the Kepler system studied in [18–22,28,29] is equivalent to our second normalized system (see Section 5.3) and to uncover the above singularity, we construct an explicit \mathbf{S}^2 map in terms of dynamical variables π_1, π_2 , and π_3 .

5.4.1. Action–angle coordinates

The Poisson algebra (47) resembles $\mathfrak{so}(3)$ and π_1, π_2 , and π_3 resemble components of an angular momentum J . More precisely, if we use $J_1 = \frac{1}{2}\pi_1$ [18–21] then (29a) suggests that π_2 and π_3 depend on the conjugate angle φ as $\cos \varphi$ and $\sin \varphi$. That this is indeed the case and that $(\frac{1}{2}\pi_1, \varphi)$ is an action–angle pair can be verified by tracing their definition back to the KS coordinates (q, p) . This has been repeatedly demonstrated [18–22,30–32] with a slight difference that our more general situation requires an adjustment of the (q, p) coordinates to ensure that π_4 and π_1 are diagonal. The transformation performing this adjustment is given by the symplectic matrix

$$U_\chi = \frac{1}{\sqrt{2}} \begin{pmatrix} R_\chi & \cdot & \cdot & \cdot \\ \cdot & R_\chi^T & \cdot & \cdot \\ \cdot & \cdot & R_\chi & \cdot \\ \cdot & \cdot & \cdot & R_\chi^T \end{pmatrix} \begin{pmatrix} 1 & 0 & 0 & 0 & -1 & 0 & 0 & 0 \\ 0 & 1 & 0 & 0 & 0 & 1 & 0 & 0 \\ 0 & 0 & 1 & 0 & 0 & 0 & -1 & 0 \\ 0 & 0 & 0 & 1 & 0 & 0 & 0 & 1 \\ 1 & 0 & 0 & 0 & 1 & 0 & 0 & 0 \\ 0 & -1 & 0 & 0 & 0 & 1 & 0 & 0 \\ 0 & 0 & 1 & 0 & 0 & 0 & 1 & 0 \\ 0 & 0 & 0 & -1 & 0 & 0 & 0 & 1 \end{pmatrix}, \tag{54a}$$

where R_χ is the 2×2 rotation matrix

$$R_\chi = \begin{pmatrix} \cos \chi & \sin \chi \\ -\sin \chi & \cos \chi \end{pmatrix}, \tag{54b}$$

and angle χ is related to α and β in (7),

$$\alpha = \cos 2\chi, \quad \beta = \sin 2\chi. \tag{54c}$$

In the new KS coordinates

$$\pi_4 = \frac{1}{2}(-n_1 + n_2 - n_3 + n_4), \quad \pi_1 = \frac{1}{2}(-n_1 + n_2 + n_3 - n_4), \tag{55}$$

where $n_i = \frac{1}{2}(q_i^2 + p_i^2)$ are actions of the four oscillators. The other components of T and V are quadratic forms in new (q, p) which are independent of α, β and can be substituted into the definition of π_2 and π_3 in (25b) and (25c). After (q, p) are replaced by

$$q_i = \sqrt{2n_i} \sin \phi_i, \quad p_i = \sqrt{2n_i} \cos \phi_i, \quad i = 1, \dots, 4,$$

we obtain

$$\pi_2 = X \cos \varphi, \quad \pi_3 = X \sin \varphi, \quad \varphi = -\phi_1 + \phi_2 + \phi_3 - \phi_4, \quad (56)$$

where $X^2 = \prod_{i=1}^4 (2n_i)$ equals (48b) and φ is the angle conjugate to $\frac{1}{2}\pi_1$ in (55).

5.4.2. \mathbf{S}^2 map of the reduced phase space P_c

The manner in which the authors of [18–21,28,29] map the second normalized (\mathbf{S}^1 symmetric) system on a sphere is described as follows. The longitude coordinate φ is introduced in (56). We choose axis π_1 as vertical, use (29b), and define the latitude θ so that

$$J_1 = \frac{1}{2}\pi_1 = \frac{1}{2}(n - |c|) \cos \theta. \quad (57a)$$

Substituting (57a) into (48b) gives

$$X^2 = \sin^2 \theta^2 (n - |c|)^2 [(n + |c|)^2 - \pi_1^2]. \quad (57b)$$

It follows that the two other components must be

$$J_2 = \frac{1}{2} \frac{\pi_2}{((n + |c|)^2 - \pi_1^2)^{1/2}}, \quad J_3 = \frac{1}{2} \frac{\pi_3}{((n + |c|)^2 - \pi_1^2)^{1/2}}. \quad (57c)$$

The map

$$P_{n,c} \rightarrow S^2 : (\pi_1, \pi_2, \pi_3) \rightarrow (J_1, J_2, J_3)$$

is, obviously, singular at $c = 0$ and $\pi_1 = \pm 1$, where it compensates for the singularity of $P_{n,c}$. Using (47) we can easily verify that J_i do indeed generate an $\mathfrak{so}(3)$ algebra, $\{J_i, J_j\} = \varepsilon_{ijk} J_k$, with Casimir

$$J^2 = J_x^2 + J_y^2 + J_z^2 = \frac{1}{4}(n - |c|)^2, \quad (58)$$

and are, therefore, components of the angular momentum J .

However, interesting and historically important the map of $P_{n,c}$ onto \mathbf{S}^2 is, it is of limited value in our study because it hides the singularity of $P_{n,c=0}$ (while bringing the $(1 - 4J_z^2)^{1/2}$ singularity into the Hamilton function $\mathcal{H}_{\text{snf}}(J; c = 0)$). Due to the singularity of $P_{n,c=0}$ all \mathbf{S}^1 symmetric perturbed Kepler systems are *qualitatively* different from the rotating rigid body. In technical terms, there is little if any simplification to gain from the transfer of the classical or quantum system to a \mathbf{S}^2 while both the classical equations of motion on $P_{n,c}$ (Section 5.3.3) and quantization of \mathcal{H}_{snf} present no special problems.

5.5. Classical studies of the crossed fields system based on the second average

In 1987 van der Meer and Cushman [25] considered the orbiting dust system and showed that the qualitative analysis of this perturbed Kepler system should be based on second normalization. This, of course, is true for the analogous crossed fields system (see Section 1.3.1). A complete analysis [27] based on the \mathcal{H}_{snf} reveals that for different relative strengths of the electric and magnetic fields all qualitatively different possible behaviours envisaged

in [25] occur in this latter system. The original system of [25] is qualitatively equivalent to the case of the weak magnetic field where $b/a > 1$ (Fig. 9, right).

Second normalization of the crossed fields system was recently implemented (independently from [25]) by von Milczewski et al. [35–37]. In fact these authors performed the same simple averaging as described in Section 3.1, and their result Ω differs from our \mathcal{H}_{snf} by a factor. They also implemented intuitively a \mathcal{EM} -like mapping which they called “adiabatic diagram” (Figs. 1, 9 and 11 of [35–37]). A comparison of our results to those of [35–37] shows how strikingly close physicists can get to uncovering profound geometric properties when relying on correct intuition and substantial experience in their analysis of concrete Hamiltonian systems. It also shows how important it is to complement “traditional” methods of analysis by mathematical techniques such as singular reduction, invariant theory, and basic concepts from differential geometry and differential topology presented from a practical point of view in Refs. [25,26].

The authors of [35–37] focused on a particular type of motion whose trajectories either begin or end (or both) at the origin $r = 0$ in the physical 3-space because this type of motion is visible in the experiments on the real quantum system [59–61]. In the regularized system, trajectories pass through the origin $q = 0$ in 4-space when the angular momentum vanishes, see (10a)–(10f). We can easily find the image of the constant level set $L = 0$ in the reduced phase space $P_{n,c}$. From definitions (15), (25a)–(25f) and, of course, restrictions (12a), (12b), (29a) and (29b) we find that when $L = 0$

$$\pi_1 = \alpha K_1, \quad \pi_2 = (2 - \alpha^2)K_1^2 + (c^2 - n^2), \tag{59a}$$

while

$$K_1^2 \leq n^2 - \frac{c^2}{1 - \alpha^2}, \quad |c| \leq \beta n. \tag{59b}$$

When $\alpha \neq 0$ this gives a parabola

$$\pi_2 = \frac{2 - \alpha^2}{\alpha^2} \pi_1^2 + (c^2 - n^2). \tag{59c}$$

Note that the $L = 0$ level set in $P_{n,c}$ depends on the orientation of T_1 defined by the parameter α . Consequently, for each given value of $T_1 = c$ the $L = 0$ set should be considered together with corresponding level sets of the second reduced Hamiltonian function $\mathcal{H}_{\text{snf}}(\alpha)$. As can be seen in Fig. 11, the \mathbf{Z}_2 -symmetric relative equilibrium

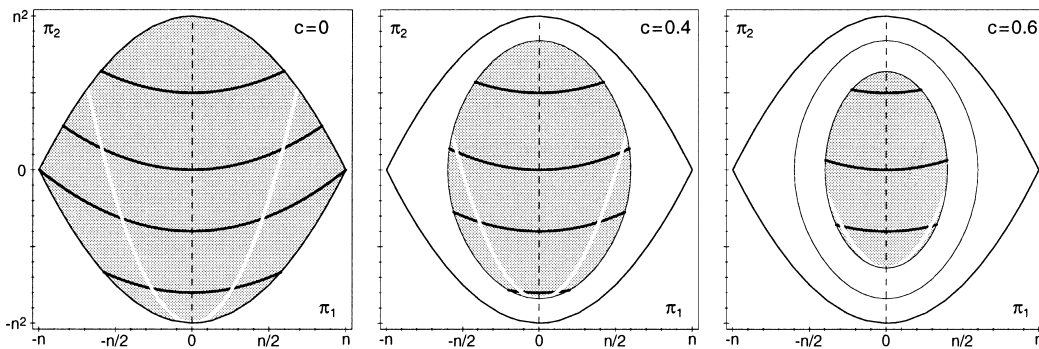


Fig. 11. Representation of the $L = 0$ level set on the reduced phase space $P_{n,c}(\pi_3 = 0)$ projection). Constant level sets of $\tilde{\mathcal{H}}_{n,0}$ with $b/a = -0.4$ ($\alpha \approx 0.684$) are shown by bold black lines while the $L = 0$ set is shown by a white line. This set is present for $|c|/n \leq \sqrt{1 - \alpha^2} \approx 0.729$.

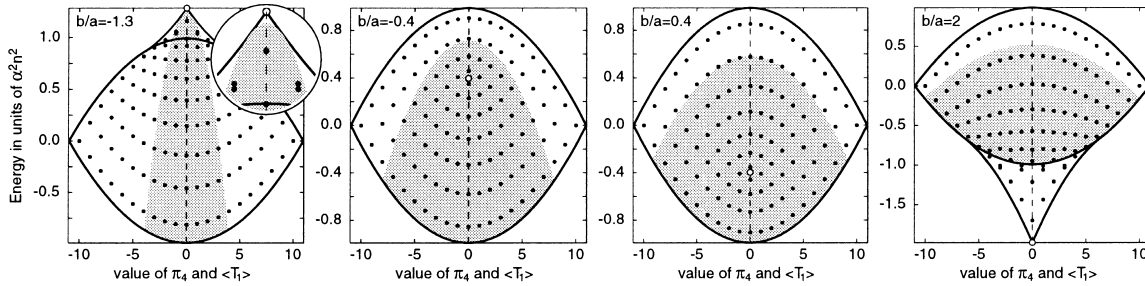


Fig. 12. Invariant subspaces intersecting the $L = 0$ set (shaded area) in the image of the energy–momentum map for different parameters b/a . Quantum number n and classical value n_{cl} are the same as in Fig. 9.

with $\pi_1 = \pi_3 = 0$ and $\pi_2 < 0$ belongs to the $L = 0$ set when c satisfies (59b). The \mathbf{Z}_2 symmetry of the equilibrium corresponds to σ_2 in (30a)–(30c) and corresponding motion is restricted to the reflection plane (Q_2, Q_3) in the initial physical 3-space.

We can see in Fig. 11 that other level sets of \mathcal{H}_{snf} intersect the $L = 0$ set in four (or two) points on $P_{n,c}$, or do not intersect it at all. The corresponding trajectories are not, of course, restricted to the plane (Q_2, Q_3) . The level set corresponding to the doubly pinched torus has four $L = 0$ points. Similar study can be done for other values of c and the results can be represented in the image of the \mathcal{EM} map. At each c the upper and lower limits of the values h of \mathcal{H}_{snf} such that $\{\mathcal{H}_{\text{snf}} = h\} \cap \{L = 0\} \neq \emptyset$ are defined by $K_1 = 0$ (relative equilibrium) and maximum $|K_1|$ (maximum π_2 of the $\{L = 0\}$ level set, see intersection $\{L = 0\} \cap \{\pi_3 = 0\}$ in Fig. 11), where the value of \mathcal{H}_{snf} reaches

$$\frac{\mathcal{H}_{\text{snf}}}{\alpha^2 n^2} = -(1+b)(1+a) \frac{c^2}{n^2 \beta^2} + 1 + b - a.$$

In Fig. 12 the image of all level sets of \mathcal{H}_{snf} which intersect the $L = 0$ set is shown by the shaded area. This is precisely the representation used in [35–37].

The geometry of the system is not analysed in [35–37] and monodromy is not uncovered. The authors do not reconstruct the inverse image of \mathcal{EM} albeit for an interesting special case resulting in a periodic orbit (Fig. 9a and 10a of [35–37]) and do not even relate the four relative equilibria of the first normalization (already introduced in [33,34]) to the singularities in the image of \mathcal{EM} . Thus the two equivalent equilibria with $(\pi_1, \pi_2, c) = (\pm 1, 0, 0)$ are missing in the analysis in Section IIIA of [35–37] even though the singularity of Ω_D in their Fig. 1 clearly indicates their presence and, in fact, the presence of the doubly pinched torus.

5.6. Comparison with early quantum calculations

Analysis of the quantum crossed fields problem goes back to 1983 when Solov'ev [38] analysed the energy level system using an n -shell second order perturbation theory. He realized that the first order problem remained degenerate (indeed, for a given value of m which Solov'ev calls $q = n' + n''$, there are $n - m$ states with the same first order correction $\varepsilon \langle T_1 \rangle$). He proceeded by diagonalizing his second order correction on the subspace of n -shell functions with fixed m (Section 3 of [38]). His resulting zeroth order equivalent operator Λ_q (Eq. (10) of [38]) is a direct quantum analogue of the second normal form $\mathcal{H}_{n,c}$ (33) obtained by averaging \mathcal{H}_{inf} along the orbits of X_{T_1} .

Later Braun and Solov'ev [42] calculated quantum energies for Λ_q of [38] in essentially the same way as we do above. Using the field strength ratio as a parameter they distinguished three different domains of the parameter

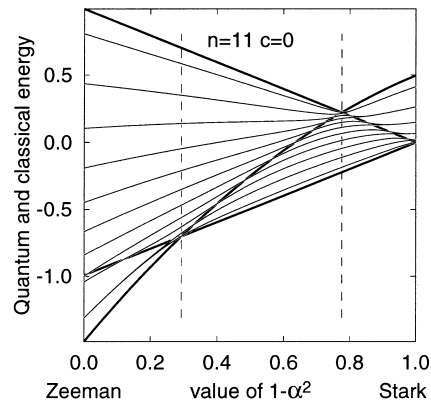


Fig. 13. Correlation diagram. Thin lines show the evolution of quantum energies (eigenvalues of the matrix of $\mathcal{H}_{n,c}$) with quantum number $n = 11$ and $\langle T_1 \rangle = 0$ between the Zeeman and Stark limits. Bold lines represent the energy of relative equilibria of $\mathcal{H}_{n,c}$ with classical value $n_{cl} = \sqrt{120}$ and $c = 0$. Dashed lines mark the monodromy interval \mathcal{I} .

values, including the one which we call the monodromy interval \mathcal{I} (34). The two relative equilibria corresponding to the singular points on $P_{n,0}$ appeared as singularities of the effective semiclassical “potential” $U(k)$ shown in Fig. 5 of [42]. When the value of the scaled field parameter α^2 was contained in the interval \mathcal{I} , the authors associated these singular points with a “quasibarrier”.

Fig. 13 illustrates the analysis of the energy level system carried out by authors of Ref. [42] (cf. Fig. 4). Since the energy level structure is analysed separately for each c (or m), monodromy cannot be seen in this way. On the other hand, one can clearly observe the correspondence between the quantum spectrum and the energies of relative equilibria shown by bold lines. These lines give the limits of the quantum spectrum. In addition, they show the threshold at which doublets of levels (corresponding to the double well 2-oscillator) appear/disappear near the Stark and the Zeeman limit (to compare with the pure Zeeman limit see Figs. 2 and 3 of [49]).

6. Discussion

We have demonstrated explicitly that the problem of hydrogen atom in orthogonal (crossed) magnetic and electric fields has the nontrivial property of monodromy. Our analysis develops geometric techniques which allow monodromy to be studied in other problems involving the hydrogen atom in fields. We have paid proper attention to the singularities of the second reduced phase space.

Our work raises a number of important questions. We have relied on normalization and attempted to extend the phenomenon of monodromy to systems which are nonintegrable in principle but which still have most of their KAM tori intact. Since this phenomenon is associated with the global organization of the whole family of invariant tori, we have assumed that it is stable under small perturbations and have demonstrated that as such it exists in the hydrogen atom in crossed fields. At the same time, more detailed understanding of monodromy, or rather of its analogue in such systems remains to be achieved. In particular, we would be greatly interested in the analysis of local action–angle variables for the Cantor sets of KAM tori surrounding the heteroclinic tangle which corresponds to the doubly pinched torus of our integrable approximation. Since these KAM tori fit together into smooth families of tori, the monodromy present in the integrable approximation survives perturbation and as such exists in the hydrogen atom problem in orthogonal electric and magnetic fields when the parameter α lies in the interval \mathcal{I} .

A different group of questions is associated with “quantum monodromy”. Here again one should attempt to generalize our methods to quantum systems whose classical analogues are not integrable, but which can be treated within the framework of quantum perturbation theory. When applying the ideas of this paper to quantum systems, one should be aware of differences between the classical and quantum normal form algorithms [58].

Persistence of quantum monodromy under small perturbations is also a subject of study on its own. We are, nevertheless, convinced that future studies of the hydrogen atom in crossed fields will reveal the energy level structure which we obtained for the quantized integrable approximation and which is characteristic of all systems with monodromy. Such studies can answer a very interesting question of how far this structure will persist with increasing perturbation (energy).

Perturbed hydrogen atom and the crossed field system in particular [59–61] continue to attract considerable interest of experimentalists. Application of the idea of monodromy in experimental studies depends on how the above questions are answered. We think that our system will become experimentally important precisely because it can, ideally, be “tuned” in and out of the interval \mathcal{I} of field parameter α , where monodromy exists.

Acknowledgements

This work has been initiated and encouraged at the workshops organized by Dr. Mark Roberts at the Mathematics Research Centre, University of Warwick, UK, in March 1997 and 1999. The idea to phrase our discussion of quantum monodromy in terms of point defects and elementary cells of 2-lattices (Section 4) is mainly due to Prof. Boris Žhilinskiĭ [11] whom we further thank for many discussions. We also thank Prof. John Delos for his improvement of Fig. 9 and Prof. Turgay Uzer [35–37] for stimulating exchange concerning.

Appendix A

A.1. Comparison of present work with [23,56]

Note the correspondence of invariant polynomials of the \mathbf{S}^1 action on $\mathbf{S}^2 \times \mathbf{S}^2$

Refs. [23,56]	Present work
$n\mu$	π_4
$n\nu$	π_1
$n^2\xi$	$\pi_2 + \pi_4^2 - \pi_1^2$
$n^2\sigma$ in (6) of [23]	$\frac{1}{2}\pi_3$

A.2. Comparison of present work with [38]

Similar to [38] the authors of [35–37] use n -scaled approach (which is more convenient for a quantum study, cf. Section B1 of [24]) as opposed to the energy-scaling in the present paper. To higher order terms, i.e., when we set $n \approx 2/\omega$, their notation corresponds to ours as indicated below

J. von Milczewski et al. [35–37]	Present work
Field strengths B and F	G and F
$C \equiv 1$	Charge C
(x, y, z) in physical 3-space	(Q_2, Q_3, Q_1)
\mathbf{p} in physical 3-space	\mathbf{P} in (1)
KS coordinates \mathbf{u} and momenta \mathbf{P}	4-vectors q and p
ω and n	Same, see (6),(12a) and (12b)
Vectors \mathbf{L} and \mathbf{A}	L and K
Vectors \mathbf{J} and \mathbf{K}	$\frac{1}{2}(K \pm L)$
$a = 3nF/B$	$\approx \frac{f}{g} = \frac{\beta}{\alpha}$
$\tilde{\mathbf{L}}$ and $\tilde{\mathbf{A}}$	T and V in (15)
$\tilde{\mathbf{J}}$ and $\tilde{\mathbf{K}}$	x and y in (16a) and (16b)
Value of \tilde{L}_z	c , value of $T_1 = \pi_4$
Parameter $\gamma(a)$ in Eq. (25)	$\frac{b}{a} = \frac{1}{2\alpha^2} - 1 - \alpha^2$
$\Omega(\gamma)$	$\frac{b}{a}\pi_1^2 - \pi_2 = -\frac{1}{a}\tilde{\mathcal{H}}_{n,c} + \frac{b}{a}(n - c)^2$, see(33)
P_s and P_u	σ_2 -symmetric relative equilibria with $\pi_1 = 0$ and $\pi_2 = \pm(n^2 - c^2)$

A.3. Invariant polynomials for various orders of \mathcal{H}_{snf}

It can be shown using invariant theory [27] that the ring of all polynomials in $(T_1, T_2, T_3, V_1, V_2, V_3)$ which are invariant w.r.t. to the $\mathbf{S}^1 \times \mathbf{Z}_2 \times \mathbf{Z}_2$ action on $S_{n/2}^2 \times S_{n/2}^2$ is freely generated by (π_2, V_1^2, T_1) . Polynomials in the k th order of the second normal form \mathcal{H}_{snf} are of degree $k + 1$ in T s and V s. Consequently (cf. (25a)–(25f)), to third order \mathcal{H}_{snf} has the following terms

Order of \mathcal{H}_{snf}	Invariant polynomials
1	T_1
ε	π_2, V_1^2, T_1^2
ε^2	$\pi_2 T_1, V_1^2 T_1, T_1^3$
ε^3	$\pi_2 T_1^2, V_1^2 T_1^2, T_1^4, \pi_2^2, \pi_2 V_1^2, (V_1^2)^2$

References

- [1] J.J. Duistermaat, Comm. Pure Appl. Math. 33 (1980) 687.
- [2] R.H. Cushman, L.M. Bates, Global Aspects of Classical Integrable Systems, Birkhäuser, Basel, 1997, see Appendix D.
- [3] R. Cushman, Centrum voor Wiskunde en Informatica Newsletter 1, 4 (1983); see also Chapter IV of R.H. Cushman, L.M. Bates, Global Aspects of Classical Integrable Systems, Birkhäuser, Basel, 1997.
- [4] R. Cushman, J.C. van der Meer, Lecture Notes in Mathematics, Vol. 1416, Springer, Berlin, 1991, p. 26.
- [5] R. Cushman, H. Knörrer, Lecture Notes in Mathematics, Vol. 1139, Springer, Berlin, 1985, p. 12.
- [6] J.C. van der Meer, The Hamiltonian Hopf Bifurcation, Lecture Notes in Mathematics, Vol. 1160, Springer, Berlin, 1985.
- [7] L. Bates, Z. Angew. Math. Phys. 6 (1991) 837.
- [8] M. Zou, J. Geom. Phys. 10 (1992) 37.
- [9] L. Bates, R. Cushman, Meccanica 30 (1995) 271.
- [10] R.H. Cushman, D.A. Sadovskii, Europhys. Lett. 47 (1999) 1.

- [11] D.A. Sadovskii, B.I. Žhilinskiĭ, *Phys. Lett. A* 256 (1999) 235.
- [12] R. Cushman, J.J. Duistermaat, *Non-Hamiltonian monodromy*, Preprint, Utrecht, 1997.
- [13] R. Cushman, J.J. Duistermaat, *Bull. Am. Math. Soc.* 19 (1988) 475.
- [14] Vū Ngoc San, *Commun. Math. Phys.* 203 (1999) 465.
- [15] M.S. Child, *J. Phys. A* 31 (1998) 657.
- [16] M.S. Child, T. Weston, J. Tennyson, *Mol. Phys.* 96 (1999) 371.
- [17] M. Kuwata, A. Harada, H. Hasegawa, *J. Phys. A* 23 (1990) 3227.
- [18] D. Farrelly, *J. Chem. Phys.* 85 (1986) 2119.
- [19] D. Farrelly, K. Krantzman, *Phys. Rev. A* 43 (1991) 1666.
- [20] K.D. Krantzman, J. Milligan, D. Farrelly, *Phys. Rev. A* 45 (1992) 3093.
- [21] D. Farrelly, J.A. Milligan, *Phys. Rev. A* 45 (1992) 8277.
- [22] D. Farrelly, T. Uzer, P.E. Raines, J.P. Skelton, J. Milligan, *Phys. Rev. A* 45 (1992) 4738.
- [23] D.A. Sadovskii, B.I. Žhilinskiĭ, L. Michel, *Phys. Rev. A* 53 (1996) 4064.
- [24] D.A. Sadovskii, B.I. Žhilinskiĭ, *Phys. Rev. A* 57 (1998) 2867.
- [25] J.C. van der Meer, R.H. Cushman, in: H. Doebner, J. Henning (Eds.), *Proceedings of the XV International Conference on Differential Geometric Methods in Theoretical Physics*, World Scientific, Singapore, 1987, p. 403.
- [26] R.H. Cushman, in: C. K. Jones et al. (Eds.), *Dynamics Reported*, Vol. 1, New Series, Springer, New York, 1992, p. 54.
- [27] D.A. Sadovskii, Unpublished result.
- [28] T. Uzer, *Phys. Rev. A* 42 (1990) 5787.
- [29] A.R.P. Rau, L. Zhang, *Phys. Rev. A* 42 (1990) 6342.
- [30] M.J. Gourlay, T. Uzer, D. Farrelly, *Phys. Rev. A* 47 (1993) 3113.
- [31] J. von Milczewski, G.H.F. Diercksen, T. Uzer, *Phys. Rev. Lett.* 73 (1994) 2428.
- [32] J. von Milczewski, G.H.F. Diercksen, T. Uzer, *Int. J. Bifurc. Chaos* 4 (1994) 905.
- [33] E. Flöthmann, J. Main, K.W. Welge, *J. Phys. B* 27 (1994) 2821.
- [34] E. Flöthmann, K.W. Welge, *Phys. Rev. A* 54 (1996) 1884.
- [35] J. von Milczewski, D. Farrelly, T. Uzer, *Phys. Rev. Lett.* 78 (1997) 2349.
- [36] J. von Milczewski, D. Farrelly, T. Uzer, *Phys. Rev. A* 56 (1997) 657.
- [37] J. von Milczewski, T. Uzer, *Phys. Rev. E* 55 (1997) 6540.
- [38] E.A. Solov'ev, *Sov. Phys. JETP* 58 (1983) 63.
- [39] R.H. Cushman, L.M. Bates, *Global Aspects of Classical Integrable Systems*, Birkhäuser, Basel, 1997, p. 408.
- [40] Nguyen Tien Zung, *Diff. Geom. Appl.* 7 (1997) 123.
- [41] R.H. Cushman, D.A. Sadovskii, *Degenerate Hamiltonian Hopf bifurcation*, in preparation.
- [42] P.A. Braun, E.A. Solov'ev, *Sov. Phys. JETP* 59 (1984) 38.
- [43] M. Robnik, *J. Phys. A* 17 (1984) 109.
- [44] M. Robnik, E. Schrüfer, *J. Phys. A* 18 (1985) L853.
- [45] R.N. Zare, *Angular Momentum*, Wiley, New York, 1988.
- [46] L.D. Landau, E.M. Lifshitz, *Quantum Mechanics, Nonrelativistic Theory*, Chapter XV, Section 113, Pergamon Press, Oxford, 1965.
- [47] E.A. Solov'ev, *JETP Lett.* 34 (1981) 265.
- [48] E.A. Solov'ev, *Sov. Phys. JETP* 55 (1982) 1017.
- [49] D.R. Herrick, *Phys. Rev. A* 26 (1982) 323.
- [50] J.B. Delos, S.K. Knudson, D.W. Noid, *Phys. Rev. A* 28 (1983) 7.
- [51] W. Gröbner, *Die Lie–Reihen und ihre Anwendungen*, Deutscher Verlag der Wissenschaften, Berlin, 1960.
- [52] W. Gröbner, *Contributions to the method of Lie series*, Bibliographisches Institut, Mannheim, 1967.
- [53] A. Deprit, *Celest. Mech.* 1 (1969) 12.
- [54] A. Deprit, V. Lanchares, M. Iñarrea, J.P. Salas, J.D. Sierra, *Phys. Rev. A* 54 (1996) 3885.
- [55] J.P. Salas, A. Deprit, S. Ferrer, V. Lanchares, J. Palacián, *Phys. Lett. A* 242 (1998) 83.
- [56] B.I. Žhilinskiĭ, L. Michel, *Rydberg states of atoms and molecules. Basic group theoretical and topological analysis*, Preprint IHES/P/97/54, *Phys. Rep.*, in press.
- [57] H. Bateman, A. Erdélyi, *Higher Transcendental Functions*, Vol. 3, McGraw-Hill, New York, 1955 (Chapter 13.13).
- [58] M. Kummer, *Fields Inst. Commun.* 8 (1996) 35.
- [59] G. Wiebusch, J. Main, K. Kruger, H. Rottke, A. Holle, K. Welge, *Phys. Rev. Lett.* 62 (1989) 2821.
- [60] G. Reithel, H. Walther, *Phys. Rev. A* 49 (1993) 1646.
- [61] C. Neumann, R. Ubert, S. Freund, E. Flöthmann, B. Sheehy, K.H. Welge, M.R. Haggerty, J.B. Delos, *Phys. Rev. Lett.* 78 (1997) 4705.
- [62] H. Weyl, *Classical Groups, their Invariants and Representations*, Princeton University Press, Princeton, NJ, 1939.
- [63] R.P. Stanley, *Invariants of finite groups and their applications to combinatorics*, *Bull. Am. Math. Soc.* 1 (1979) 475.
- [64] B. Sturmfels, *Algorithms in Invariant Theory*, Springer, Berlin, 1993.